Sulfonated Poly(ether ketone) Grafted Multi-Walled Carbon Nanotubes

Gyung-Joo Sohn

Energy Conversion and Storage Major
Interdisciplinary School of Green Energy
Graduate School of UNIST

2012

Sulfonated Poly(ether ketone) Grafted Multi-Walled Carbon Nanotubes

Gyung-Joo Sohn

Energy Conversion and Storage Major
Interdisciplinary School of Green Energy
Graduate School of UNIST

Sulfonated Poly(ether ketone) Grafted Multi-Walled Carbon Nanotubes

A thesis
submitted to the Interdisciplinary School of Green Energy
and the Graduate School of UNIST
in partial fulfillment of the
requirements for the degree of
Master of Science

Gyung-Joo Sohn

01. 18 . 2012 [Month/Day/year of submission]

Approved by

_____

Major Advisor
Jong-Beom Baek

Sulfonated Poly(ether ketone) Grafted Multi-Walled Carbon Nanotubes

Gyung-Joo Sohn

This certifies that the thesis of Gyung-Joo Sohn is approved.

01. 18 . 2012 [Month/Day/year of submission]

signature

Thesis supervisor: Jong-Beom Baek

signature

Hyeon Suk Shin

signature

Jin Young Kim

Abstract

We report water-soluble multi-walled carbon nanotubes (MWCNT), to which sulfonated hyperbranched poly(ether-ketone) (SHPEK) is grafted. To endorse sufficient water affinity to MWCNT, dendritic hyperbranched poly(ether-ketone) (HPEK) was first covalently grafted to the surface of MWCNT via Friedel-Crafts acylation reaction. The resultant HPEK grafted MWCNT (HPEK-g-MWCNT) was subsequently sulfonated in chlorosulfonic acid to produce SHPEK-g-MWCNT, which is soluble well in water showing Zeta potential value of -57.8 mV (good stability). The SHPEK-g-MWCNT paper prepared from a simple filtration of aqueous dispersion has sheet resistance as low as 63 Ω/sq and high electrocatalytic activity for oxygen reduction reaction (ORR). Thus, the new design and synthetic methodologies suggest that water-dispersible MWCNT, which is a new class of high performance cathode material for ORR.

Contents

List of figures

List of tables

Nomenclature (Scheme)

PPA Polyphosphoric acid

P_2O_5 Phosphorous pentoxide

MWCNT Multi-walled Carbon Nanotube

NMP N-methyl-2-pyrrolidone

DMAc N,N-dimethylacetamide

HPEK Dendritic hyperbranched poly(ether-ketone)

HPEK-g-MWCNT HPEK grafted MWCNT

SHPEK-g-MWCNT Sulfonated HPEK-g-MWCNT

PET Poly(ethylene terephthalate)

Pt/C Platinum (Pt) on activated carbon

GC Glassy carbon

D.I. water Distilled water (Deionized water)

CVD Chemical Vapor Deposition

I. Introduction

Since the discovery of Carbon nanotubes (CNTs) by Sumio Iijima in 1991, carbon nanotubes have been a focal point of materials researches and developments due to their outstanding physical, electrical and thermal properties.[1] CNTs have been used for polymer-based composites,[2] energy storage such as hydrogen storage, fuel cells, and the lithium battery, composite materials,[3] electronic devices,[4] biosensors[5] and many others.[6] CNTs can be thought of as sheets of carbon rolled up into a tubular structure is called a single-wall carbon nanotube (SWCNT), and a rolled up stack of sheets results in multiwall carbon nanotubes (MWCNTs).

Although CNTs as nanoscale additives are expected to significantly improve the performances of hybrid materials, there are two critical issues addressed first for maximum enhanced properties. They are homogeneous dispersion with minimal and/or without structural distortions and strong interfacial adhesion between CNTs and supporting matrices. Hitherto, there have been many physical,[7] chemical,[8] and combined methods[9] to optimize stable dispersion of CNTs in foreign matrices. Ultrasonicaiton has been the most favorable physical method for the dispersion of CNTs. It has, however, been known to seriously damage CNT frameworks by sidewall opening, breaking and turning into amorphous carbon depending upon dose strength, time, and temperature.[10] Thermodynamic gains from enthalpy by bond dissociation and functionalization and entropy by breaking and fragmentation are primary driving force for the homogeneous dispersion upon sonication after scarifying the high crystallinity and aspect ratio of pristine CNTs. Treating corrosive and oxidative acids such as nitric acid, sulfuric acid and their mixture are the most commonly used chemical method for the functionalization of CNTs.[11] Similar to conversion of graphite into graphite oxide/graphene oxide (GO),[12] corrosive oxidation has long been exploited. The treatments of corrosive acids turn CNTs into CNT-oxides (Theoretically, CNT should be more reactive than graphite due to C-C bond strain and larger surface area). As observed in GO,[13] the electrical insulating and defective nature of CNT-oxides cannot display outstanding properties from pristine CNTs, leaving CNT researches in a back seat after graphene researches booming.[14] Even after homogeneous dispersion is achieved in common organic media to provide processability, the interaction between CNTs and supporting matrices becomes the secondary consideration for being used as reinforcing additives. Thus, considering the critical issues in CNT researches, an efficient chemical modification of CNTs without causing CNT damages and their dispersion in eco-friendly media for convenient processing still remain as an important challenge.

Hyperbranched polymers have distinctive, special chemical and physical properties, and they have played a vital role in interface and surface sciences, which can be used advantageously as functional surfaces and interfacial materials. In addition, hyperbranched polymers have good

solubility, lower melt viscosity, and extremely high density of functional groups at the surface compared with the linear analogues. Hyperbranched polymers should therefore increase the solubility of MWCNTs and enable further functionalization of MWCNTs. Most molecular wires have poor solubility and processing ability; however, when these insoluble molecular wires are wrapped with highly branched polymers, the branched polymers not only protect and stabilize the central conjugated backbone of molecular wires by preventing intermolecular actions but also improve the solubility and processability without altering their electronic characteristics. Moreover, hyperbranched polymers can be covalently modified with a broad range of functional groups, such as fluorophores, electroactive groups, perfluorinated moieties, dyes, and other linear polymers and also the surface-confined hyperbranched polymers are suitable for a number of technical applications, including corrosion inhibition, chemical sensing, cellular engineering, and micrometer-scale patterning. Therefore, hyperbranched polymers may be ideal materials to coat and functionalize carbon nanotubes.

Here, we report water-soluble multi-walled carbon nanotubes (MWCNTs), which was prepared in a simple two-step reaction. Dendritic hyperbranched poly(ether-ketone) (HPEK) was first grafted to the surface of as-received MWCNT by *in-situ* polycondentation of 3,5-diphenoxybenzoic acid as an AB_2 monomer (Figure 3) *via* "direct" Friedel-Crafts acylaton in a mild polyphosphoric acid (PPA)/phosphorous pentoxide (P_2O_5) medium.[15] The reaction medium is known to be non-corrosive and sp^2 hybrid C-H defect-selective functionalization of CNTs.[16] Dendritic macromolecules such as dendrimers and hyperbranched polymers consist of densely branched 3-dimensional structures with the large number of periphery functional groups,[17] which can be utilized for further chemical modification. Thus, the resultant HPEK grafted MWCNT (HPEK-g-MWCNT) was able to provide numerous reactive sites for subsequent sulfonation in chlorosulfonic acid. The hydrophilic nature of the sulfonated HPEK-g-MWCNT (SHPEK-g-MWCNT) expected to display water-solubility without having further damages and introducing oxygenated defects to CNT framework. In this way, CNTs could have dispersibility (processability) in desired media with preserving their aspect ratio and structural integrity. As a result, CNT-based functional materials are expected to display improved electrocatalytic performance and they are useful for eco-friendly spray coating application.

II. Experiment

2.1 Materials

All reagents and solvents were purchased from Aldrich Chemicals Inc. and used as received. Multi-walled carbon nanotubes (CVD MWCNT 95 with diameter of ~20 nm and length of 10-50μm) was obtained from Hanwha Nanotech, Incheon, South Korea.

2.2 Instrumentations

Fourier-transform Infrared (FT-IR) spectra data were recorded on a Jasco Fourier transform spectrophotometer model 480 Plus. All samples were mixed with KBr powder and pressed to make semi-transparent pellets. The data were collected in the wavelength range from 450 to 4000 cm^{-1}. Elemental analyses (EA) were performed with a CE Instruments EA1110. Zeta potential measurements were performed with Malvern Nano ZS. Thermogravimetric analysis (TGA) was conducted in air atmospheres with a heating rate of 10 °C/min using a TA Q200 thermogravimetric analyzer. Powder X-ray diffraction (XRD) measurements were carried out using a Rigaku DMax/2000PC with a Cu target tube. X-ray photoelectron spectroscopy (XPS) analysis was carried out on a Thermo Fisher K-alpha employing a monochromatic A1 Kα radiation as the X-ray source. The field emission scanning electron microscopy (FE-SEM) used in this work was FEI NanoSem 230. High resolution transmission electron microscope (HR-TEM) employed in this work was a JEOL JEM-2100F (Cs) operating at 200 kV. The HR-TEM samples were prepared by dropping solution of dispersed samples in D.I. water.

2.3 *In-situ* grafting of HPEK onto MWCNT (*STEP 1*) (Figure 1a)

Into a resin flask equipped with a high torque mechanical stirrer, nitrogen inlet and outlet, 3,5-diphenoxybenzoic acid (2.0 g, 6.53 mmol), and MWCNTs (2.0 g), polyphosphoric acid (PPA, 80.0 g, 83% P_2O_5 assay), and phosphorous pentoxide (P_2O_5, 20.0 g) was placed. The reaction flask was immersed in an oil bath and the reaction mixture was stirred under dry nitrogen purge. The flask was heated to 100 °C for 1 h and further heated to 130 °C and maintained for 72 h. The homogeneous reaction mixture was poured into distilled water and the precipitates were collected by suction filtration. The dark black solids were transferred to extraction thimble and Soxhlet-extracted with water for three days to completely remove residual reaction medium and with methanol for three more days to get rid of low-molar-mass HPEK and other possible organic impurities. Finally, the sample was freeze-dried under reduced pressure (0.5 mmHg) at -120 °C for 48 h to give 3.21 g of black powders. Free-standing high-molar-mass HPEK was further washed off by Soxhlet extraction with dichloromethane. The final product (HPEK-g-MWCNT) was freeze-dried to give 2.34 g (60.3% yield) of black powder. Anal. Calcd. For $C_{157.76}H_{13}O_3$ (calculated on the basis of yield): C, 96.91%; H, 0.66%; O, 2.42%. Found: C, 94.95%; H, 0.65%, O, 4.39%.

2.4 Sulfonation of HPEK-g-MWCNT in chlorosulfonic acid (*STEP 2*) (Figure 1b)

Into the one-necked round bottom flask equipped with a magnetic stirrer, nitrogen inlet and a dropping funnel, HPEK-g-MWCNTs (0.5 g) were placed. Chlorosulfonic acid (99%, 50 mL) was slowly added into the flask and stirred at room temperature for 4h. The reaction flask was immersed in ice bath for cooling down the temperature. After reaction, distilled water was slowly added for 1h. The precipitates, which were settled at the bottom of the flask, were collected by filtration and washed with D.I. water (50 mL) 10 times. The final product was freeze-dried -120 °C under reduced pressure (0.5 mmHg) for 48 h to give 0.55 g of dark powder. Anal. Calcd. for $C_{125.99}H_{14}O_6S_1$ (calculated on the basis of yield): C, 91.41%; H, 0.85%; O, 5.80%; S, 1.94%. Found: C, 86.21%; H, 0.76%; O, 9.03%; S, 2.07%.

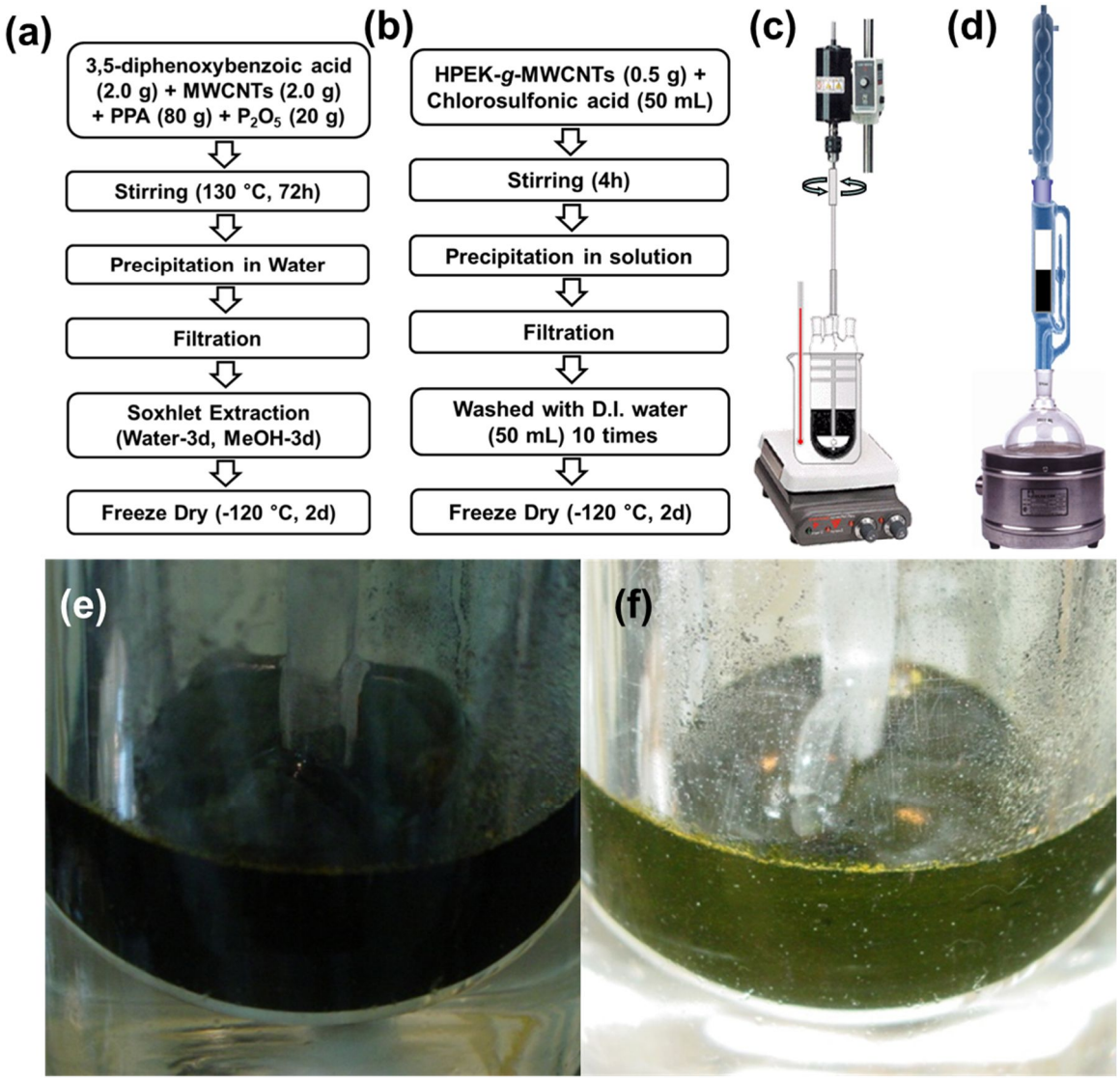

Figure 1. Experimental procedure of (a) *STEP 1* and (b) *STEP 2*. Apparatus for (c) purification, functionalization and (d) soxhlet extraction (c) photographs taken from the reaction flask of HPEK-g-MWCNT in PPA/P_2O_5: (e) without and (f) with flash light. Deep green color with flash light indicated uniform grafting of HPEK to the surface of MWCNT and homogeneous dispersion of HPEK-g-MWCNT.

III. Results and discussion

3.1 Functionalization of MWCNT

Taking advantages of the characteristic natures of three-dimensional (3-D) dendritic macromolecules,[17] water-dispersible multi-walled carbon nanotubes (MWCNTs) were prepared as rare cases.[18, 19] In order to covalently anchor dendritic macromolecules to the surface of MWCNTs and endorse hydrophilic nature, a two-step reaction sequence involving Friedel-Crafts acylation in a mild polyphosphoric acid (PPA)/phosphorous pentoxide (P_2O_5) medium and subsequent sulfonation in chlorosulfonic acid (Cl-SO_2-OH) was applied. The Friedel-Crafts acylation in a PPA/P_2O_5 medium is known to be non-corrosive and sp^2 hybrid C-H defect-selective functionalization condition and an efficient polymerization condition.[16] To estimate the inherent sp^2 hybrid C-H defects on MWCNTs for the reaction, elemental analysis (EA) was conducted (Table 1). 'Pristine' MWCNTs contain a significant amount of hydrogen (0.30 wt%, converting into atomic percent could suggest the number of available sp^2 hybrid C-H per carbons), which is attributable to the inherent sp^2 hybrid C-H defects. The result indicates an upper limit of one hydrogen atom attached for every 28 carbon atoms (Table 1). The available sp^2 hybrid C-H defects on MWCNT are anchoring sites for dendritic macromolecules in PPA/P_2O_5 medium as non-destructive functionalization *via* Friedel–Crafts acylation reaction. The reaction medium, PPA with an optimized amount of P_2O_5, is benign not to damage MWCNT but strong enough to selectively functionalize at the sp^2 hybrid C-H defects. PPA is a viscous polymeric acid, which can provide strong shear to promote efficient dispersion of CNTs during mechanically stirring and to impede reaggregation after dispersion. In addition, it has a mild acidity (pK_a = ~ 2.1), which is about the same as gastric acid (pK_a = 1.3~3.5), not to oxidize and damage CNT framework.[15, 16] Thus, PPA has many advantages for functionalization of carbon-based nanomaterials over the commonly used corrosive acids such as nitric acid (pK_a = -1.5)/sulfuric acid (pK_a = -3.0) mixture for the synthesis of CNT-oxides.[20] The role of P_2O_5 is removal of water molecule, which is generated as by-product from the dehydration of carboxylic acid during the course of Friedel-Crafts reaction. As described in Figure 3, the reaction between P_2O_5 and water results in increasing molecular weight of PPA, not allowing backward reaction but only forward reaction. In order to covalently graft hyperbranched poly(ether-ketone) (HPEK) to the surface of MWCNTs, the AB_2 monomer, 3,5-diphenoxybenzoic acid, was synthesized as following literature report (SHU, C. F., LEU, C. M. & HUANG, F. Y. 1999. Synthesis, modification, and characterization of hyperbranched poly(ether ketones). *Polymer*, 40, 6591-6596.). FT-IR clearly confirm the presences of keto-carbonyl band at 1659 cm^{-1}, C-O-C band at 1267 cm^{-1}, symmetrical of epoxy ring at 1270 cm^{-1} (Figure 4). Pristine MWCNT was grafted with HPEK by *in-situ* polymerization of the monomer in a PPA/P_2O_5 medium

to produce HPEK-g-MWCNT (Figure 2, chemical structures of monomer and HPEK-g-MWCNT are delineated in Figure 5).[21] The viscosity of the reaction mixture was increased as grafting of HPEK to the surface of MWCNT proceeded (Figure 1e). Interestingly, the photograph of the reaction mixture showed dark-green color with flash light (Figure 1f), indicating that HPEK was uniformly grafted to the surface of MWCNT and the resultant HPEK-g-MWCNT was homogeneously dispersed in the reaction medium. The dark powder that precipitated upon pouring into distilled water was collected by suction filtration and washed with water. To minimize unexpected variables, the product was completely worked up by Soxhlet extraction with water and methanol to remove the reaction medium and low molar mass impurities, respectively. It was further washed with dichloromethane, which is good solvent for HPEK, to get rid of freestanding HPEK and dried to give 60.3% yield. Elemental analysis (EA) determined on the basis of yield is in good agreement between theoretical and experimental CHO counts (Table 1).

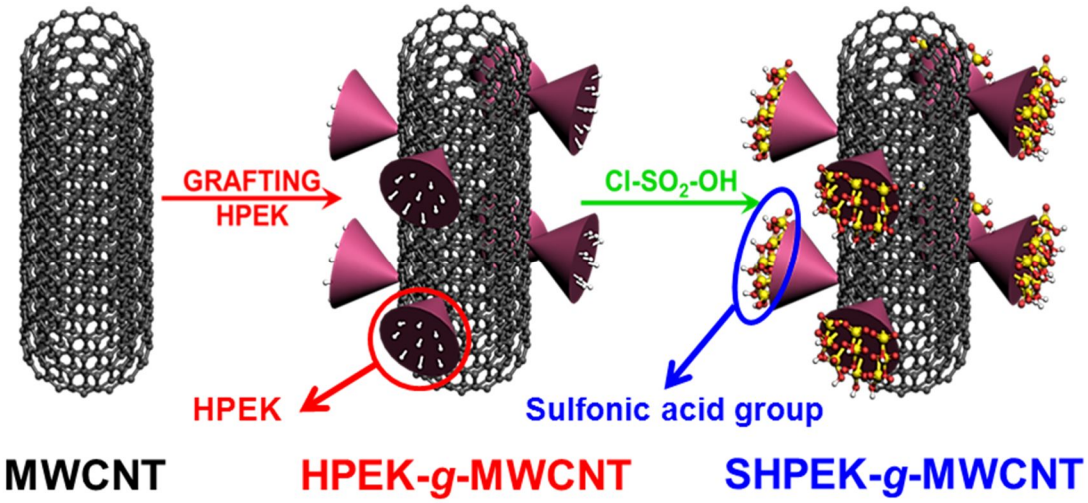

Figure 2. Schematic demonstrations for the covalent grafting of HPEK to the surface of MWCNTs in PPA/P_2O_5 medium and subsequent sulfonation of HPEK-g-MWCNT in chlorosulfonic acid to yield SHPEK-g-MWCNT.

Table 1. Elemental analysis of pristine MWCNT, HPEK-g-MWNCT and SHPEK-g-MWCNT

Sample		Elemental Analysis					
		C (%)	H (%)	O (%)	S (%)	C/H	C/S
Pristine MWCNT	Calc.	100.0	0.0	0.0	0.0		
	Found	98.2	0.3	BDL*	0.0	28	
S-MWCNT	Found	96.12	0.13	1.90	0.30		855
HPEK-g-MWCNT	Calc.	96.91	0.66	2.42	0.0		
	Found	94.95	0.65	4.39	0.0		
SHPEK-g-MWCNT	Calc.	91.41	0.85	5.80	1.94		
	Found	86.21	0.76	9.03	2.07		85

* BDL = below detection limit.

The HPEK-g-MWCNT was subsequently sulfonated in chlorosulfonic acid to produce sulfonated HPEK-g-MWCNT (SHPEK-g-MWCNT) (Figure 2). For comparison, direct sulfonation of pristine MWCNT in chlorosulfonic acid was also carried out in the same reaction condition for the synthesis of SHPEK-g-MWCNT. Resultant sulfonated MWCNT (S-MWCNT) (Figure 6a) has only 1 sulfonic acid per 855 carbons (C/S = 855, see Table 1). As a result, the S-MWCNT is not soluble in water, indicating that the degree of direct sulfonation is not high enough to affect the surface nature of S-MWCNT. Thus, to provide enough reactive sites for sulfonation, grafting of dendritic HPEK onto the surface of MWCNT will dramatically increase reactive sp^2 hybrid C-H sites. The minimum number of available ortho- and para-positioned sp^2 hybrid C-H to ether-activated phenyl are tremendously increased to n(DP+1),[17] where n is an average number of HPEK's covalently attached to MWCNT and DP stands for an average degree of polymerization (Figure 6b). The sulfonation of HPEK-g-MWCNT introduces a large number of sulfonic acids to the periphery of HPEK-g-MWCNT and makes SHPEK-g-MWCNT hydrophilic enough to be soluble well in water.[5] The SHPEK-g-MWCNT has 1 sulfonic acid per 85 carbons (see, Table 1). The degree of sulfonation was increased almost 10 times as high as that of S-MWCNT. Due to the sulfonic acids in water being *c.a.* ~100% dissociated and negatively charged,[22] the SHPEK-g-MWCNT is indeed dispersible well in polar aprotic solvents such as *N,N*-dimethylacetamide (DMAc) and *N*-methyl-2-pyrrolidone (NMP). It is also well soluble in polar protic solvents such as methanol, ethanol and water (Figure 7).

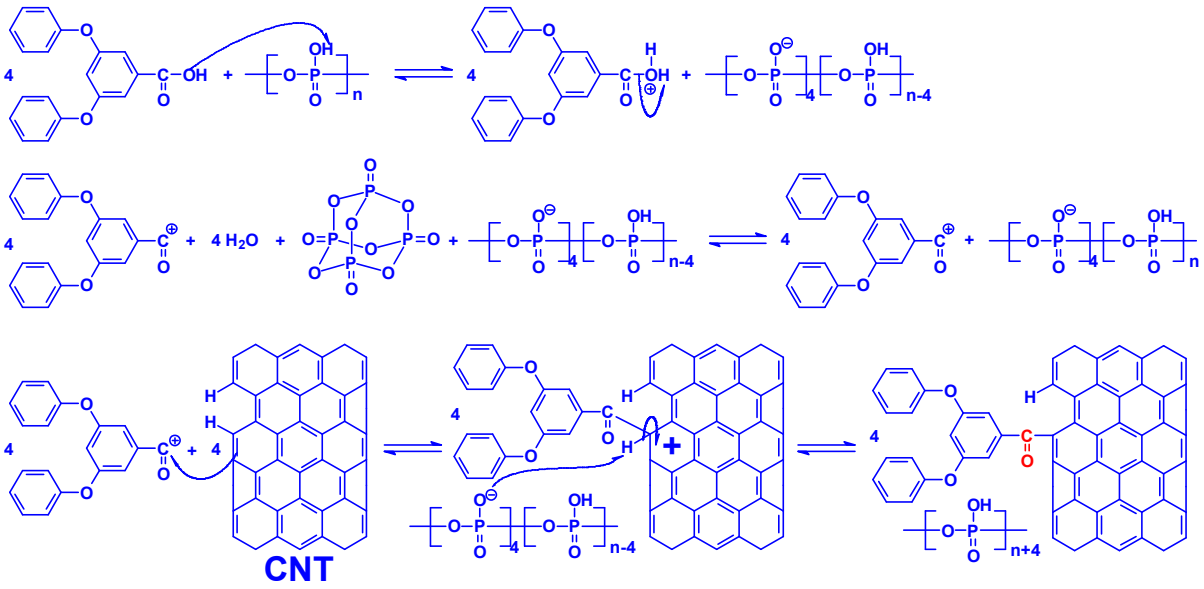

Figure 3. Proposed mechanism of Friedel-Crafts acylation reaction in PPA/P_2O_5 medium, showing defect-selectively grafting of AB_2 monomer to the site of sp^2 hybrid C-H on CNT defects (The structure of CNT was simplified for easy understanding).

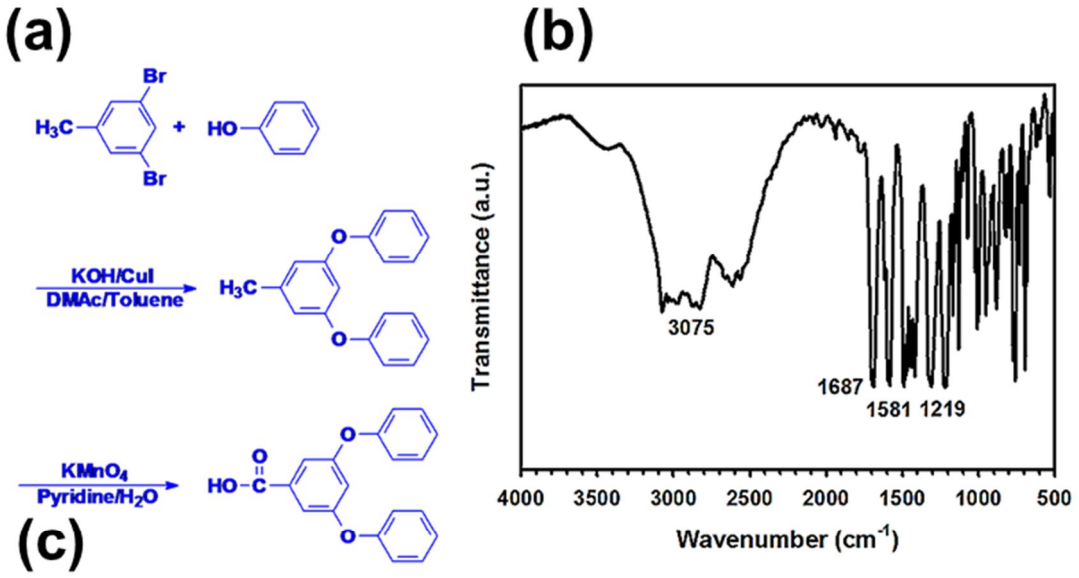

(c)

Sample		C (%)	H (%)	O (%)
3,5-diphenoxybenzoic acid	Calc.	74.50	4.61	20.89
	Found	74.42	4.58	20.95

Figure 4. (a) Synthesis of AB_2 monomer, 3,5-diphenoxybenzoic acid, starting from 3,5-dibromotoluene and phenol; (b) FT-IR spectrum (KBr pellet) of 3,5-diphenoxybenzoic acid; (c) elemental analysis of pure 3,5-diphenoxybenzoic acid.

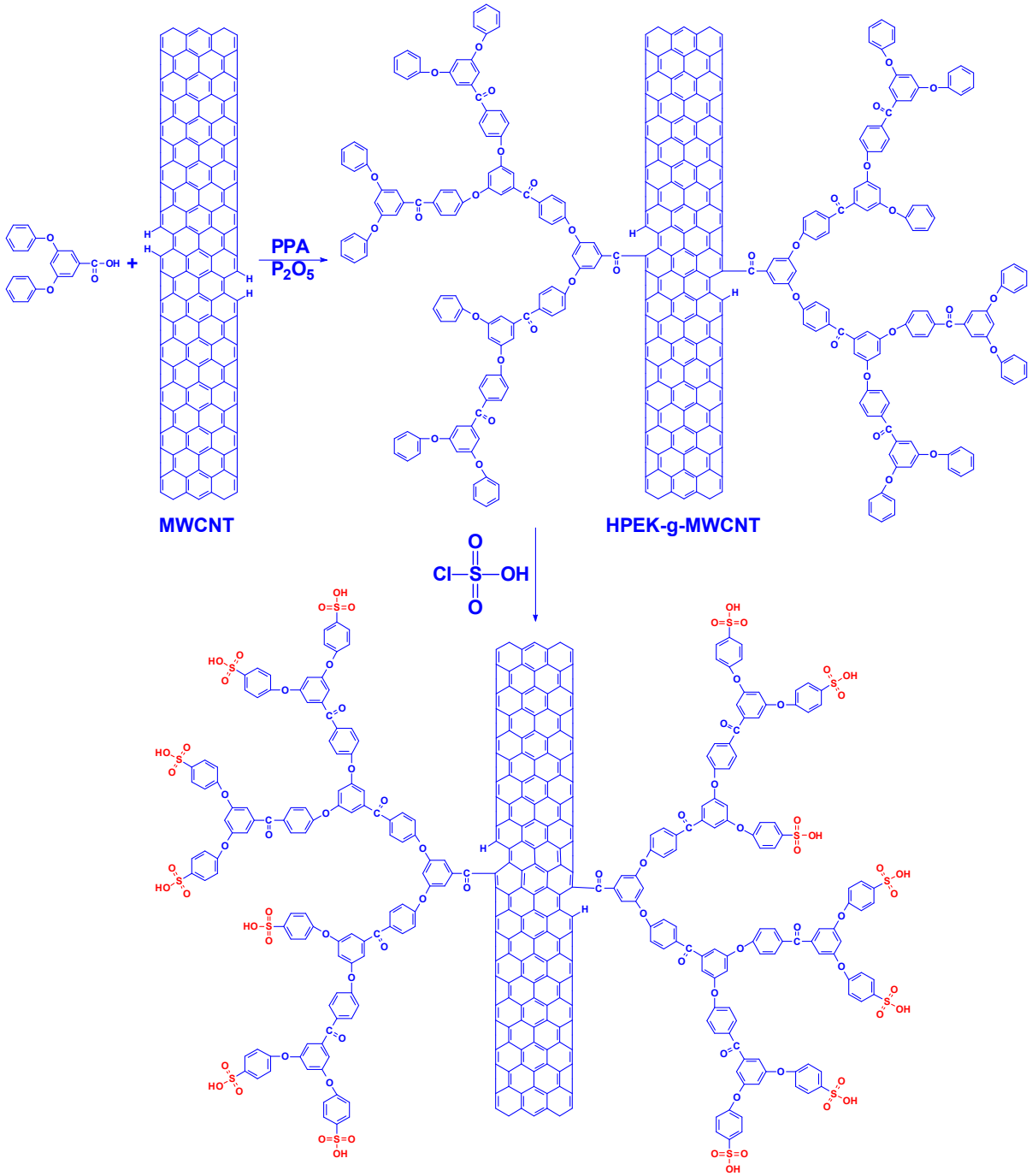

Figure 5. Schematic presentation of HPEK grafted MWCNT (HPEK-g-MWCNT) in PPA/P_2O_5 medium and subsequent sulfonation of HPEK-g-MWCNT in chlorosulfonic acid to produce sulfonated HPEK-g-MWCNT (SHPEK-g-MWCNT).

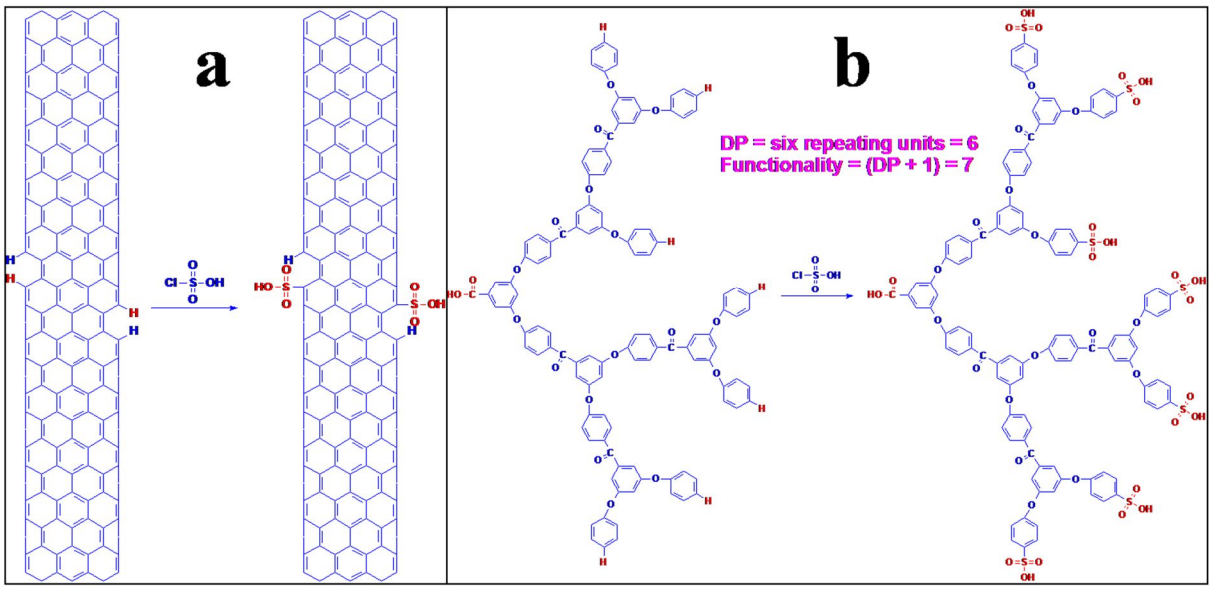

Figure 6. (a) Direct sulfonation of MWCNT in chlorosulfonic acid to yield sulfonated MWCNT (S-MWCNT). The sulfonation should be to the site of sp^2 hybrid C-H on MWCNT defects; (b) the structure of HPEK with six repeating units (the degree of polymerization (DP) = 6) and sulfonation of HPEK in chlorosulfonic acid. The available reactive sites for the sulfonation are DP + 1 = 7. Thus, grafting HPEK to the surface of MWCNT could increase as much as average number of HPEK molecules (*n*) per MWCNT multiplied by average degree of polymerization (DP) + 1, i.e., *n*(DP + 1). For example, if *n* is 10 and DP is 99, *n*(DP + 1) becomes 1000. As a result, 1000 of sulfonic acids could be introduced to the HPEK-g-MWCNT to produce SHPEK-g-MWCNT, which could provide enough hydrophilicity for water dispersion.

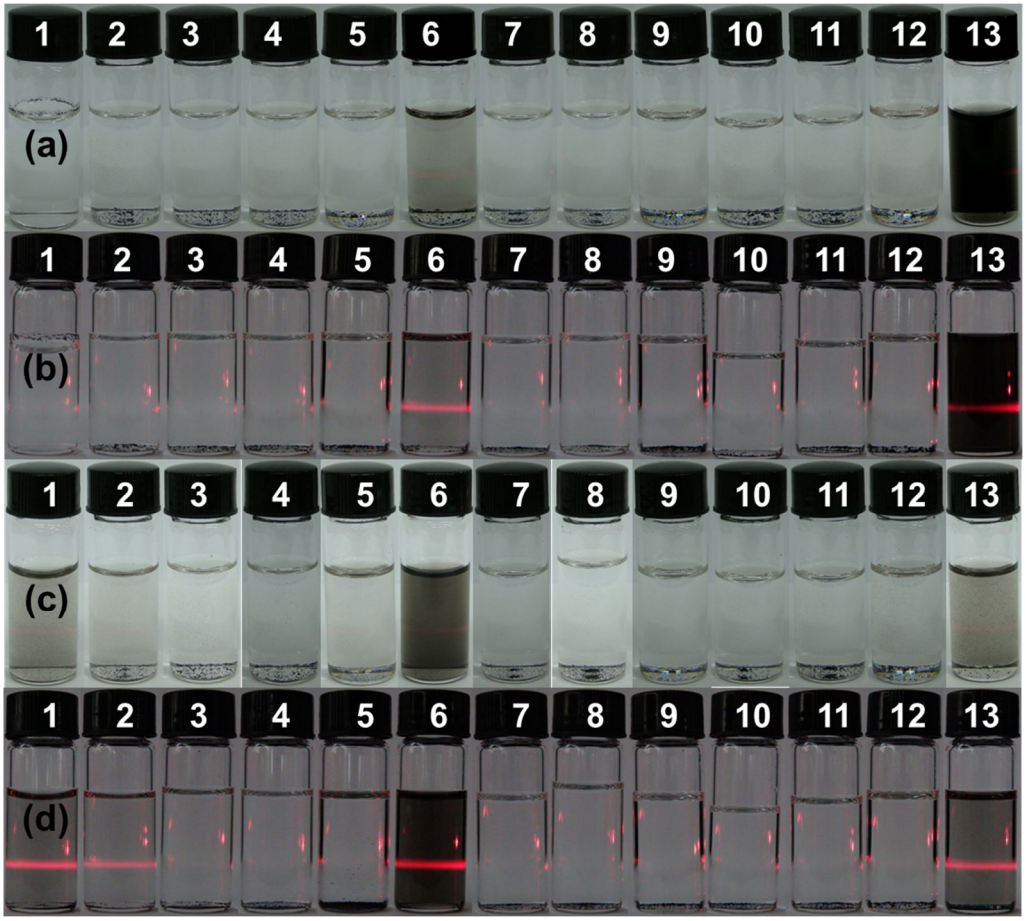

Figure 7. Photographs of samples dispersed in different solvents: (a) as-prepared HPEK-g-MWCNT solutions with hand held laser shining; (b) HPEK-g-MWCNT solutions after one week at ambient condition with hand held laser shining; (c) as-prepared SHPEK-g-MWCNT solutions with hand held laser shining (d) SHPEK-g-MWCNT solutions after one week at ambient condition with hand held laser shining. (1) distilled water, (2) methanol, (3) ethanol, (4) acetic acid, (5) toluene, (6) DMAc, (7) heptane, (8) acetone, (9) benzene, (10) dichloromethane, (11) THF, (12) pyridine, and (13) NMP.

3.2 Zeta Potential Study

Zeta potential indicates the difference in electrical potential between the particle and the liquid in which it moves. For molecules and particles that are small enough, a high zeta potential value confer stability, *i.e.* the solution or dispersion will resist aggregation. When the potential is low, attraction exceeds repulsion and the dispersion will break and flocculate.

The electrophoretic mobility of the particles, i.e. the speed which they achieve in an electric field, is linearly related to their zeta potential. The Zetasizer indeed measures zeta potential by timing particle speed in an electric field. The particle suspension is injected into a "folded capillary cell" (figure 8a), equipped with electrodes on both sides, and the particle speed down the applied electric field, is monitored with a laser beam. (figure 8b)

ASTM (American Society for Testing and Matrials) defines colloids with zeta potentials. Particles with zeta potentials more positive than +40mV or more negative than -40mV are considered stable. The pristine CNTs shows low zeta potential value (−8.3 mV in References).[22] The aqueous dispersion of SHPEK-g-MWCNT (17.4 mg in 500 mL water) shows -57.8 mV (Figure 9), whose value is considered to be a “good stability” of colloidal dispersion (Table 2) and the lowest value for carbon-based nanomaterials among reported by far.[23, 24]

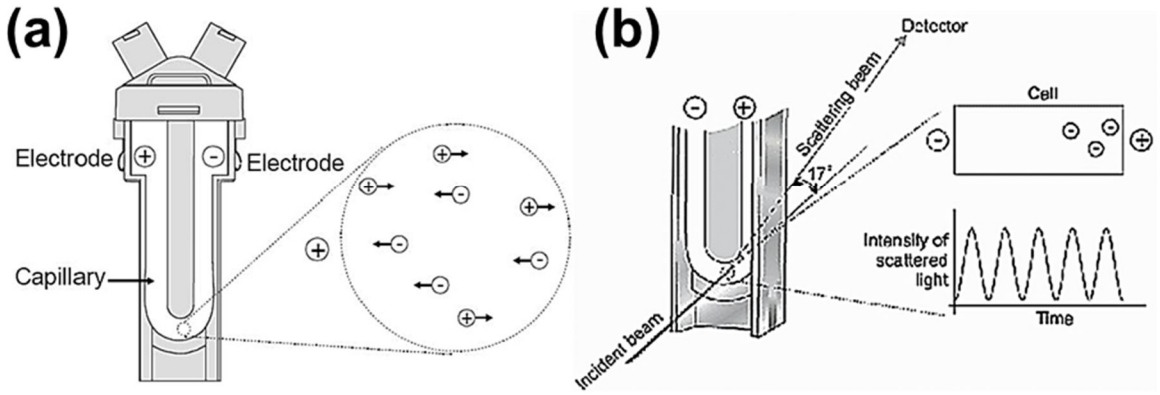

Figure 8. (a) Zeta potential cell stuructre and (b) detection of zeta potential inside of the cell.

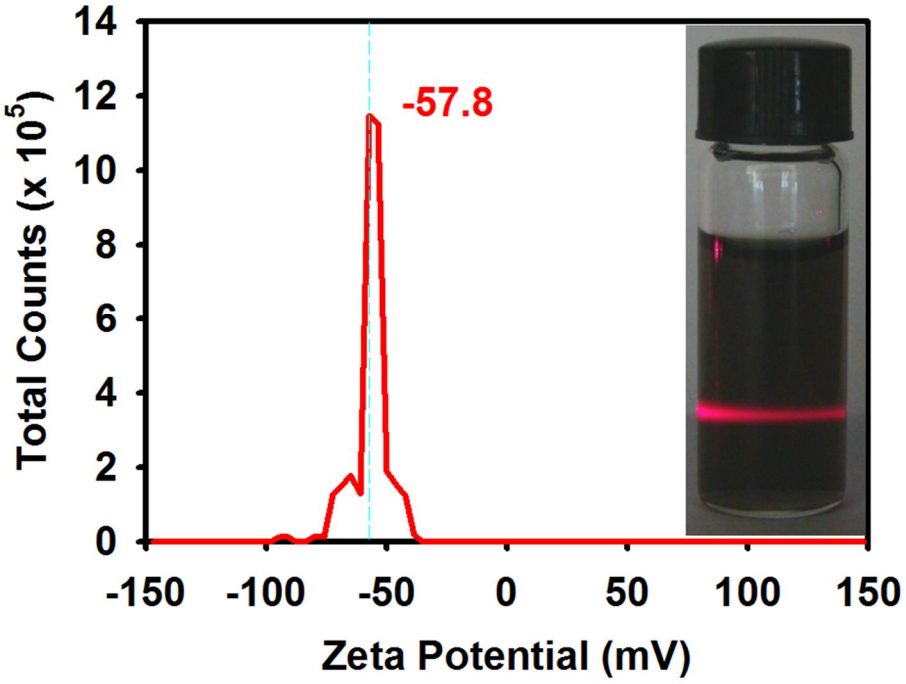

Figure 9. Zeta potential curve of SHPEK-g-MWCNT (17.4 mg) solution in water (500 mL). Inset is photograph of the solution with hand held laser shinning.

Table 2. The relationship between Zeta potential and colloidal stability.

Zeta Potential [mV]	Stability behavior of the colloids
from 0 to ±5	Rapid coagulation or flocculation
from ±10 to ±30	Incipient instability
from ±30 to ±40	Moderate stability
from ±40 to ±60	Good stability
more than ±61	Excellent stability

3.3 Fourier Transform Infrared Spectroscopy

To ensure the covalent attachment of HPEK to the HPEK-g-MWCNT and sulfonic acids on SHPEK-g-MWCNT, samples were subjected to FT-IR analysis. Spectra from HPEK-g-MWCNT and SHPEK-g-MWCNT exhibit absorption peaks at 2918 and 2842 cm^{-1} corresponding to sp^2 hybrid C-H and sp^3 hybrid C-H stretching bands, respectively. And also they show aromatic carbonyl (C=O) at 1731cm^{-1}. C=C ring stretch adsorptions occurred in pairs at 1640 and 1383 cm^{-1}, respectively (Figure 10). The strong hydroxyl stretching vibrations appeared at 3435 cm^{-1} is moisture present in KBr. SHPEK-g-MWCNT shows characteristic S=O and S-O stretching bands at 1263 and 1100-1027 cm^{-1}, respectively, and a peak at 805 cm^{-1} is assignable to C-S vibration. The result is clear evidence for sulfonic acids on SHPEK-g-MWCNT.

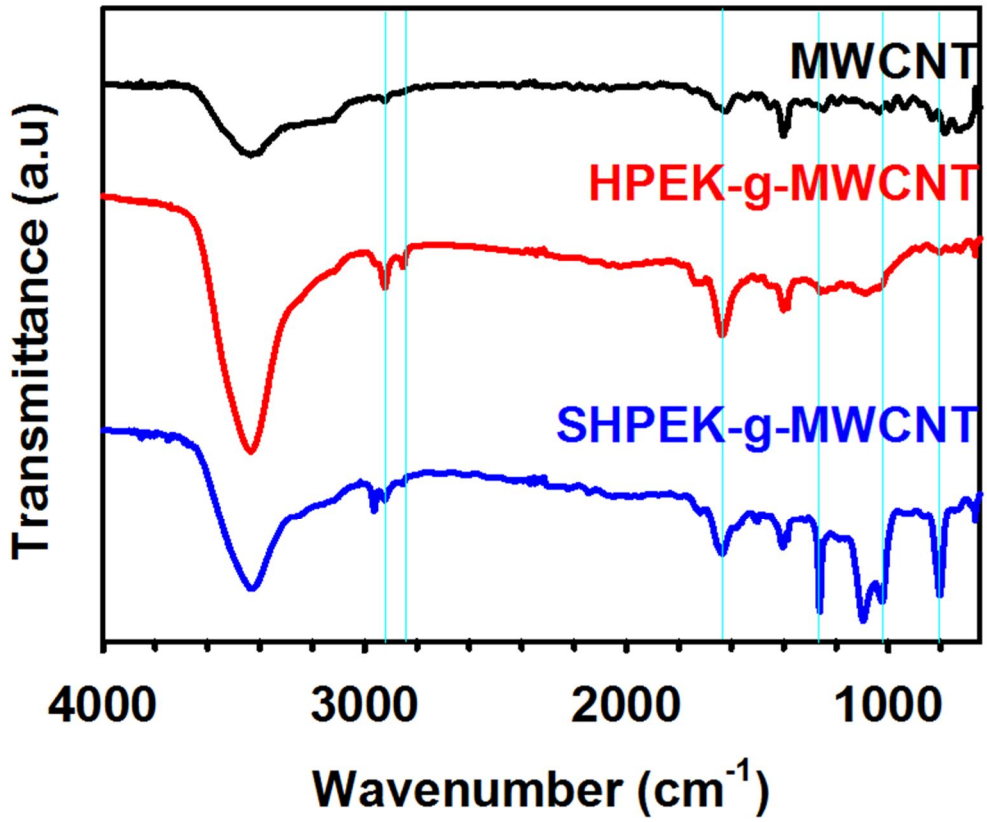

Figure 10. FT-IR (KBr pellet) spectra: 'Pristine' MWCNT, HPEK-g-MWCNT and SHPEK-g-MWCNT.

3.4 Thermal Properties

Thermal stabilities of MWCNT, HPEK-g-MWCNT and SHPEK-g-MWCNT are shown in Figure 11. The samples were heated in the chamber of thermogravimetric analyzer (TGA) to 800 °C with the ramping rate of 10 °C/min for experiments conducted in air . MWCNT, HPEK-g-MWCNT and SHPEK-g-MWCNT showed that the temperature at which 5% weight loss ($Td_{5\%}$) in air occurred at 584, 461 and 380 °C (Table 3). Unmodified pristine MWCNT displayed the highest thermo-oxidative stability. HPEK-g-MWCNT and SHPEK-g-MWCNT displayed similar thermal behavior, stepwise weight loss. The temperature difference at which 5% weight loss ($Td_{5\%}$) means the thermo-oxidative stability between these samples. It is caused by the fact that the polymeric moiety covalently attached to the surface of MWCNTs was thermally stripped off, causing early weight loss. In other wise, the thermal stability of the polymer decreases with increasing number of chain ends. The amount of polymer attached on the surface of MWCNT can be expected by these results. In the case of HPEK-g-MWCNT, the weight loss occurred in the temperature range from 470 to 600 °C is related to HPEK covalently attached to the surface of MWCNTs. The amount of HPEK grafts is approximately 25 wt%. In the case of SHPEK-g-MWCNT, two-step weight loss was observed. The initial weight loss started from 330 to 470 °C, which could be attributable to the decomposition of sulfonic acids in the form of SO_3,[25] was approximately 10 wt%. The second step weight loss from 470 to 600 °C should be originated from the decomposition of HPEK moiety, which was thermooxidatively stripped off from MWCNT surface in air.[22] In all cases, char yields at 800 °C approached to zero, indicating that there were almost no persisting metallic impurities that presented in MWCNT (vide infra).

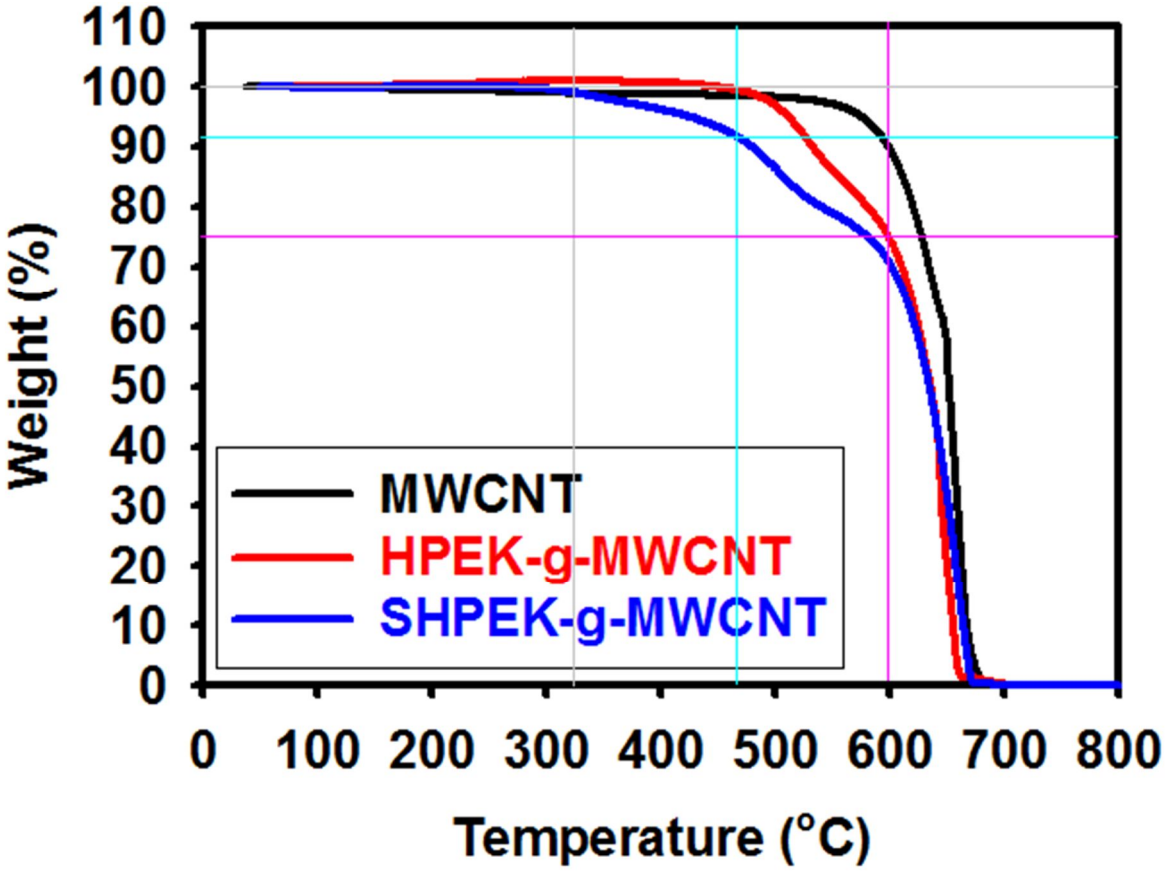

Figure 11. TGA curves of 'Pristine' MWCNT, HPEK-g-MWCNT and SHPEK-g-MWCNT with heating rate of 10 °C/min in air.

Table 3. The 5% weight loss of MWCNT, HPEK-g-MWCNT and SHPEK-g-MWCNT.

Sample	$T_{d5\%}$
MWCNT	584
HPEK-MWCNT	511
SHPEK-MWCNT	429

3.5 Wide-angle X-ray diffraction (WAXD)

To determine the morphologies of HPEK-g-MWCNT and SHPEK-g-MWCNT, as-prepared powder samples were subjected to Wide-angle X-ray diffraction (WAXD) scans. Wide-angle X-ray diffraction (WAXD) was also proved the role of the reaction medium, PPA/P_2O_5. If the reaction condition and work-up procedures could damage MWCNT framework, its crystallinity should be diminished. However, the peak intensities at 25.54°, which is related to wall-to-wall distance of MWCNT, were increased as reaction steps increased (Figure 12). The result suggests that grafting and sulfonation reactions are purifying rather than damaging MWCNT.[17, 21] The decreased intensities of residual metallic impurities (denoted by *), which would be attributed to the detachment of metallic particles from the MWCNT. The HPEK-g-MWCNT does not show peaks from residual catalysts and displayed d-spacing values at 3.48 Å (2θ = 25.54°), 2.12 Å (2θ = 42.64°) and 1.72 Å (2θ = 53.19°). SHPEK-g-MWCNT displayed d-spacing values at 3.44 Å (2θ = 25.9°), 2.10 Å (2θ = 42.96°) and 0.96 Å (2θ = 53.25°).

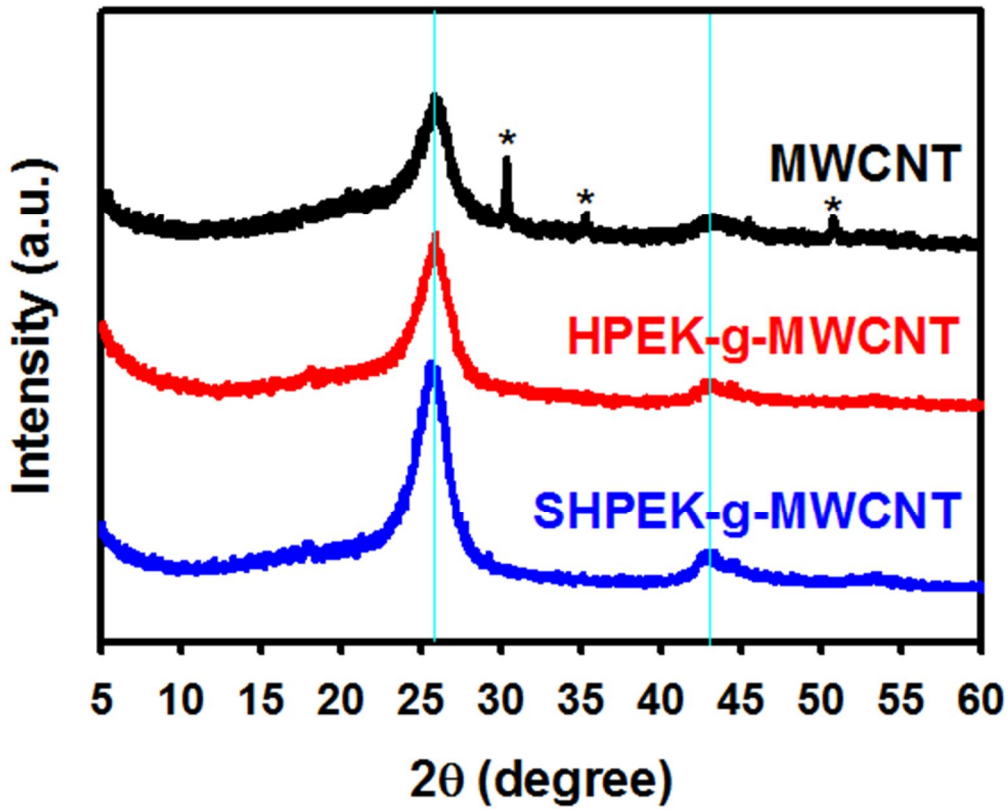

Figure 12. WAXD patterns : 'Pristine' MWCNT, HPEK-g-MWCNT and SHPEK-g-MWCNT.

3.6 X-ray photoelectron spectroscopy (XPS)

The X-ray photoelectron spectroscopy (XPS) survey of pristine MWCNT shows a strong C 1s peak at 284.5 eV and a very weak O 1s at 533.0 eV (Figure 13a), which is mainly attributable to physically adsorbed oxygen to the surface of graphitic carbon.[26] The HPEK-g-MWCNT also displays a strong C 1s peak at 284.5 eV and relatively stronger O 1s peak due to the contribution from carbonyl (C=O) and ether (-O-) in HPEK together with physically adsorbed oxygen (Figure 13a). In the case of SHPEK-g-MWCNT, XPS spectrum displays typical C 1s and O 1s peaks at 284.5 and 533.0 eV, respectively (Figure 13b). Due to the sulfonic acids on its periphery, SHPEK-g-MWCNT shows characteristic S 2p and S 2s peaks at 168.3 and 232.4 eV, respectively (Figure 13b, insets).[27] The S 2p peak is assignable to S $2p_{3/2}$ electron, confirming an efficient sulfonation of HPEK to convert SHPEK.

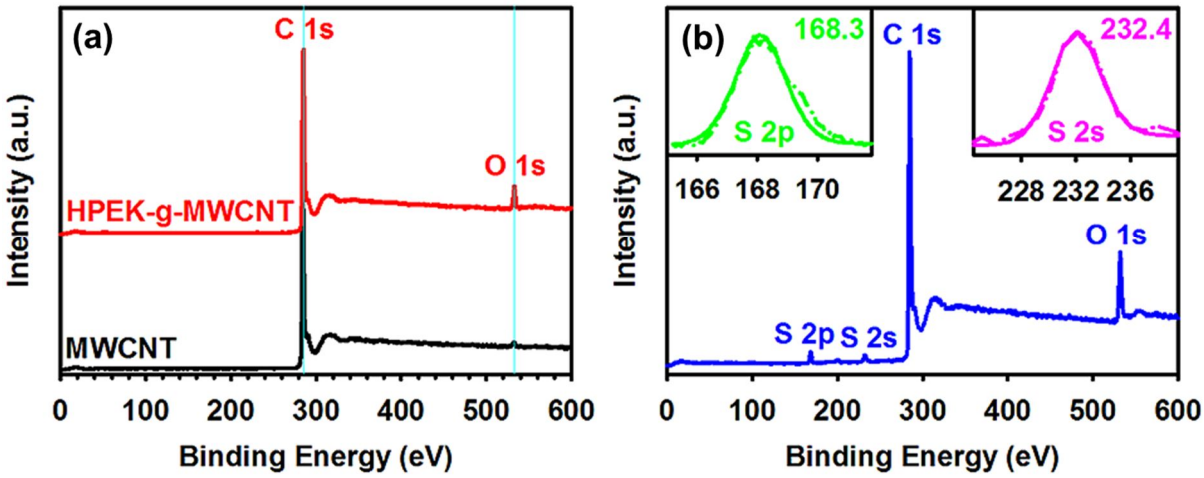

Figure 13. XPS spectra: (a) 'Pristine' MWCNT and HPEK-g-MWCNT; (b) SHPEK-g-MWCNT. Insets are S 2p (left) and S 2s (right) peaks.

3.7 Scanning electron microscopy

SEM images were obtained from HPEK-g-MWCNT and SHPEK-g-MWCNT. Pristine MWCNT has tube diameter and length in the range of 10-20 nm and 10-50 μm, respectively, showing spaghetti-like network with smooth and clean surface. Due to the HPEK and SHPEK coats on MWCNT, overall tube diameter dimensions of HPEK-g-MWCNT and SHPEK-g-MWCNT are increased to 30-40 nm, while their tube lengths remain almost constant (Figure 14b and 14d). Furthermore, there are no freestanding HPEK and SHPEK observed, implying that freestanding polymers were completely washed off during workup procedures (multiple Soxhlet extraction). In conjunction with TGA, the results strongly suggest that HPEK has been uniformly grafted onto the surface of MWCNT and efficiently sulfonated HPEK to SHPEK. Furthermore, SEM element mapping clearly displays the uniform distribution of corresponding elements (Figure 15a-15d). Energy dispersive X-ray spectroscopy (EDX) was used as an additional information to confirm the S concentration on the surface of MWCNT (Figure 16), confirming that C, O and S are uniformly distributed. The weight percent of S was detected as high as 4.7 wt% (inset table of Figure 16), whose value is more than twice of that from EA result (2.07%, Table 1). The discrepancy may be originated from the sensitivity difference between two methods. EDX is known to be more regionally sensitive to the chemical composition.[28] Thus, EA result would be more reliable for quantitative estimation of element contents in bulk state. HPEK-g-MWCNT consists of C, H and O, while SHPEK-g-MWCNT is composed of C, H, O and S. The sole presence of S in SHPEK-g-MWNCT indicates that a significant number of sulfonic acids have been introduced to the surface of the SHPEK-g-MWCNT (see Table 1).

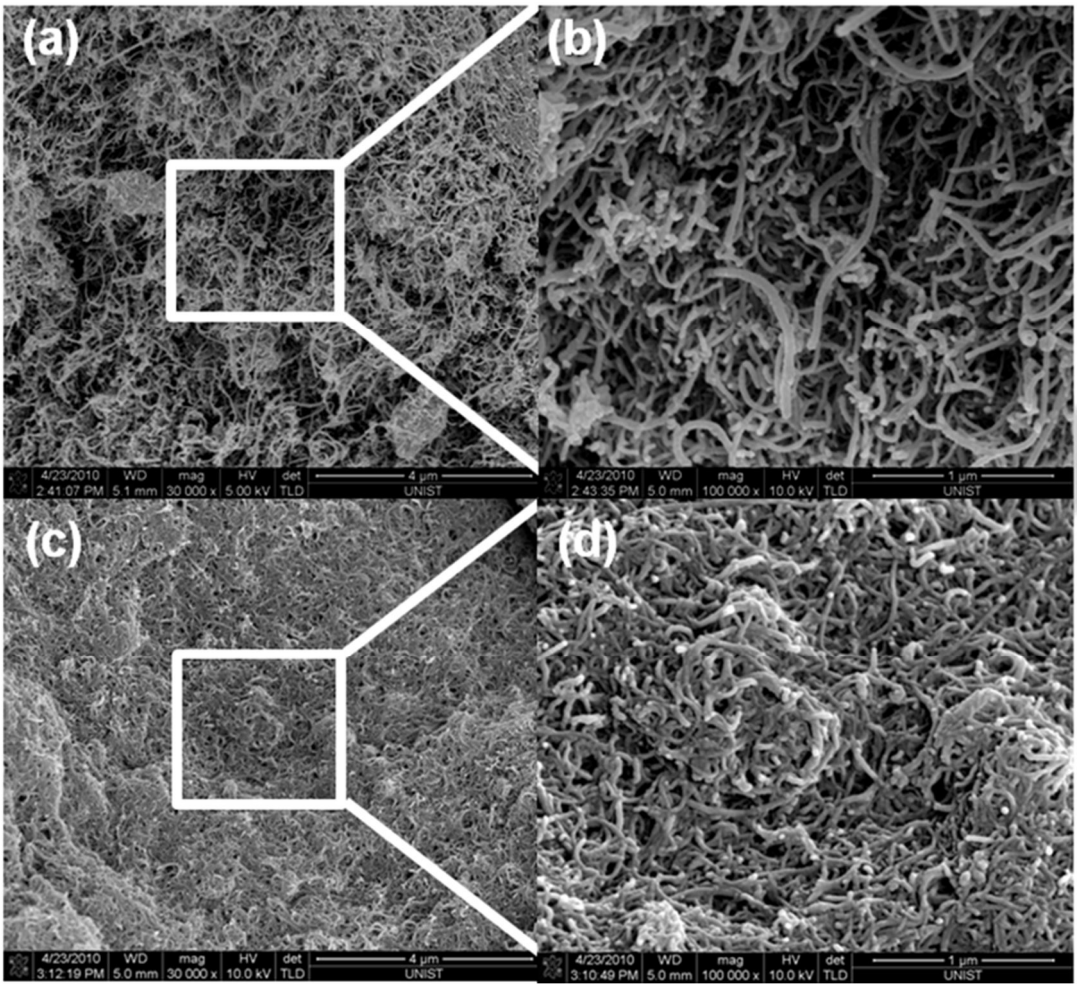

Figure 14. SEM images of (a) HPEK-g-MWcNT (30,000x), (b) HPEK-g-MWCNT (100,000x) ,(c) SHPEK-g-MWCNT (30,000x) and (d) SHPEK-g-MWCNT. (100,000x)

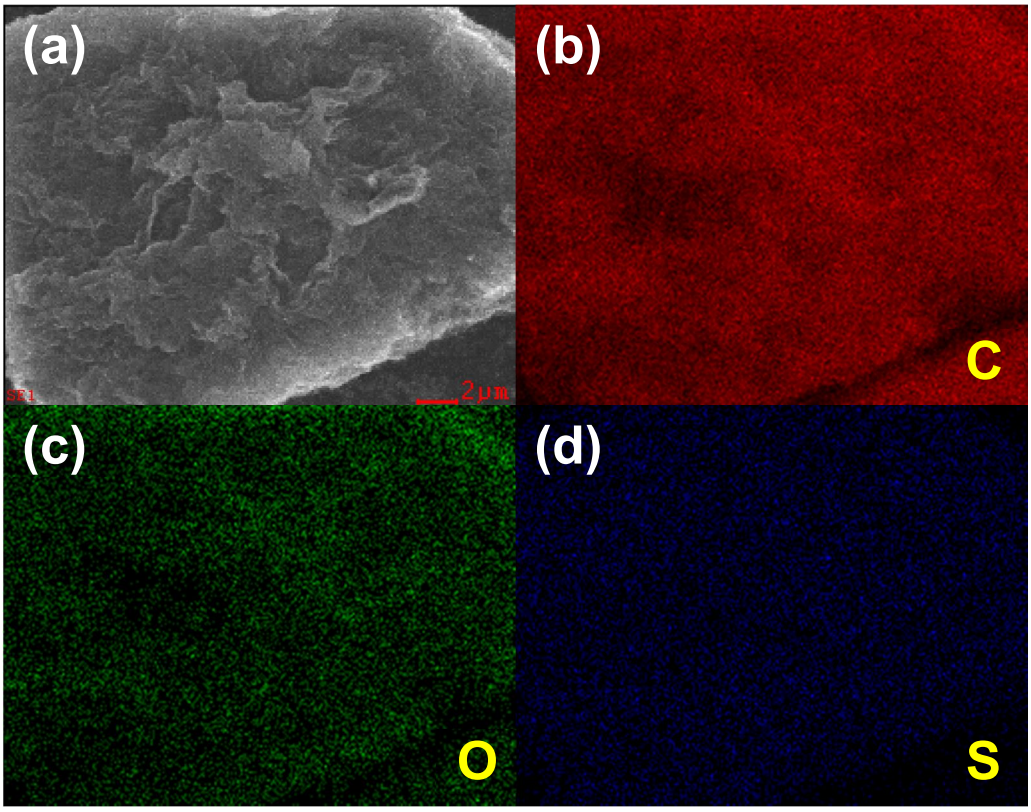

Figure 15. (a) Scanning SEM image of SHPEK-g-MWCNT; (b) elemental mapping of C present in part a; (c) elemental mapping of O present in part a; and (d) elemental mapping of S present in part a.

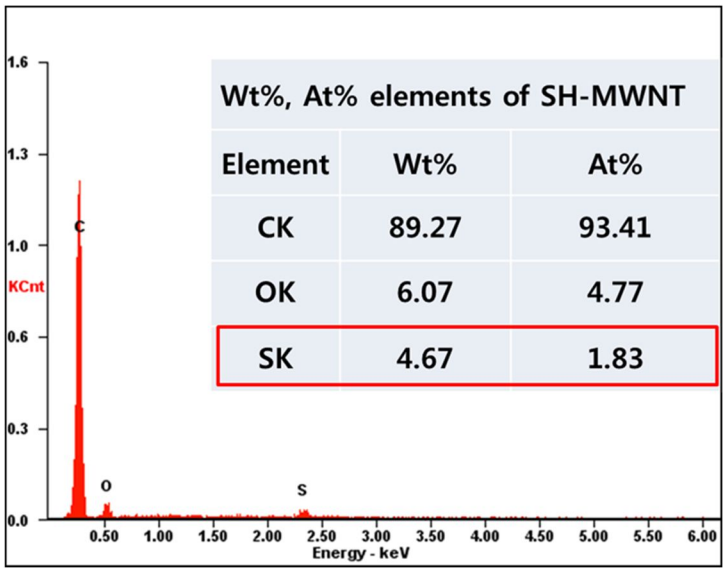

Figure 16. EDS spectrum and each Wt% and At% of SHPEK-g-MWCNT elements.

3.8 Transmission electron microscopy

In order to further visually assure the uniform grafting and subsequent sulfonation, the dispersed solutions of pristine MWCNT, HPEK-g-MWCNT and SHPEK-g-MWCNT in ethanol were very much diluted. The solutions were dropped to the carbon coated grid and vacuum-dried. The surface of pristine MWCNT is clean and smooth with clear stripes originated from its high crystalline graphitic walls. In the case of HPEK-g-MWCNT, inner core MWCNT is uniformly decorated by HPEK outer layer with thickness of ~2 nm (Figure 17a). Similarly, the out-most layer of SHPEK-g-MWCNT is coated by SHPEK with thickness of ~4 nm (Figure 17b). The increase in thickness of SHPEK layer compared to HPEK is due possibly to intramolecular charge repulsion between sulfonic acids. The stripes of inner cores implicate that MWCNTs of HPEK-g-MWCNT and SHPEK-g-MWCNT remain structurally intact during reactions and work-up procedures.

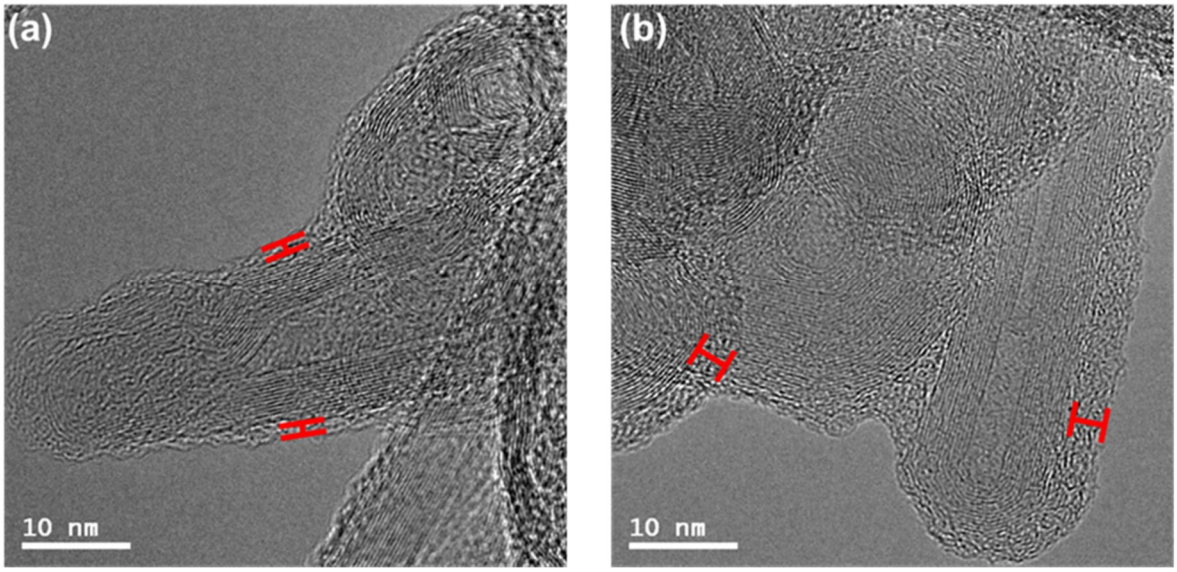

Figure 17. TEM images: (a) HPEK-g-MWCNT; (b) SHPEK-g-MWCNT.

3.9 Spray Coating of SHPEK-g-MWCNT on PET

SHPEK-g-MWCNT showd good dispersibility in the distilled water. PET (Poly(ethylene terephthalate)) can be used as a bendable substrate. First, SHPEK-g-MWCNT was dispersed in the distilled water and the concentration was 0.5 mg/ml. Before spray coating, PET films was UV plasma treated for making hydrophilic surface. After each cycle, 1 layer was coated on the PET film and for complete drying, there was 30 seconds term between each cycle. Five samples were made and each number of cycles are 100,125,150,175 and 200 at 55 °C. (Figure 18 and Figure 19)

The optical transmittances of SHPEK-g-MWCNT coated on PET (SHPEK-g-MWCNT/PET) were determined by using UV-vis spectroscopy (Figure 20a). The sheet resistances of the films were measured with four-point probe and averaged at ten different locations. The relation between sheet resistance and optical transmittance is shown in Figure 20b. SHPEK-g-MWCNT/PET films show sheet resistance in the ranges of 33-180 kΩ/sq with optical transmittance of 63-79% at 550 nm. The approach demonstrates a unique wet-chemical functionalization of pristine MWCNT, which does not require oxidative damage onto CNT framework and makes MWCNT soluble in water. The SEM images were obtained from the top view of the SHPEK-g-MWCNT coated PET films. PET films were uniformly coved with SHPEK-g-MWCNT. (Figure 21 and Figure 22)

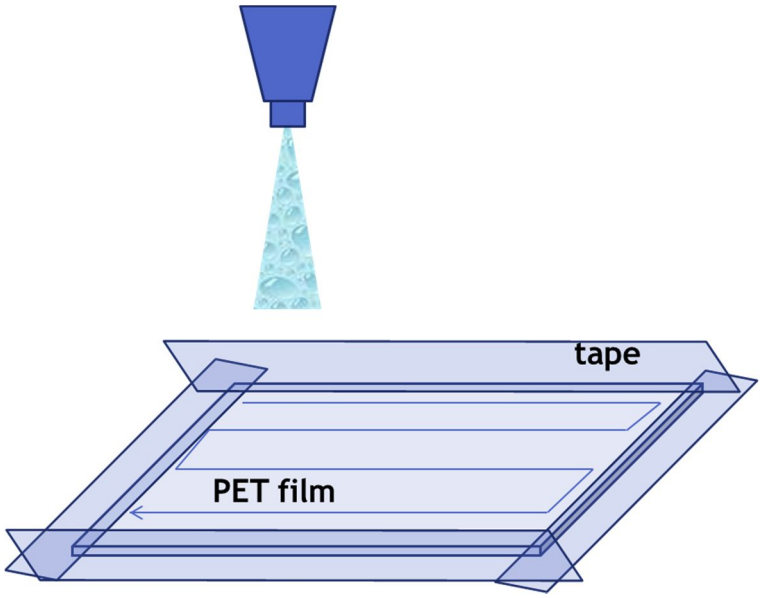

Figure 18. Schematic presentation of spray coating.

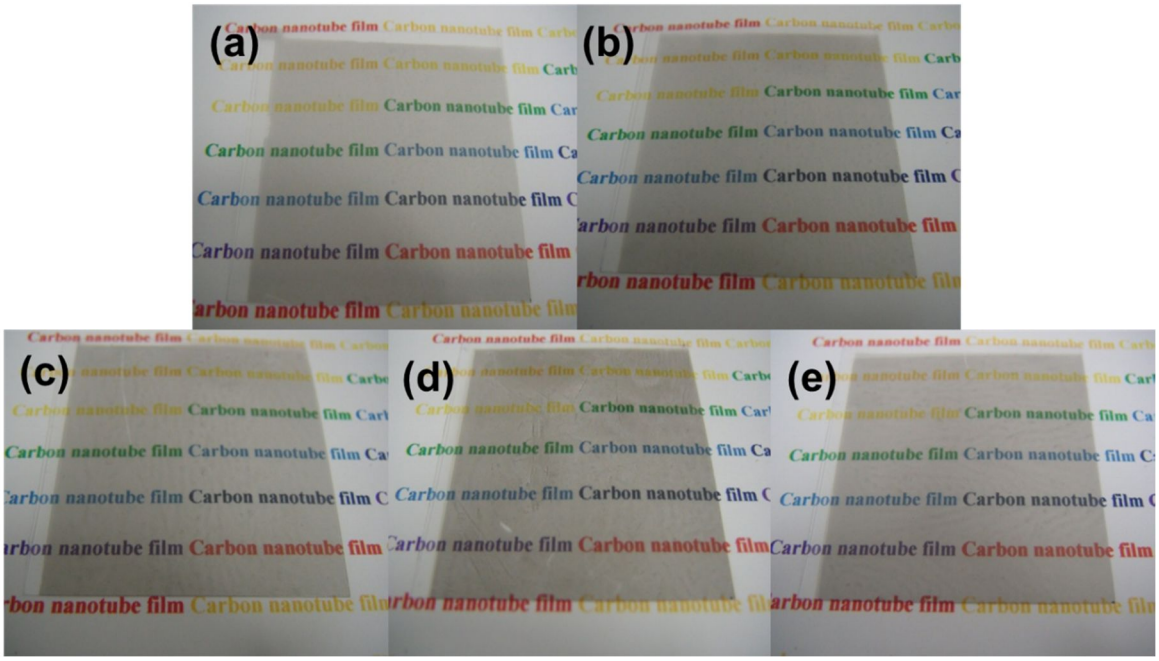

Figure 19. Photographs of (a) 100 spray coatings; (b) 125 spray coatings; (c) 150 spray coatings; (d) 175 spray coatings; (e) 200 spray coatings.

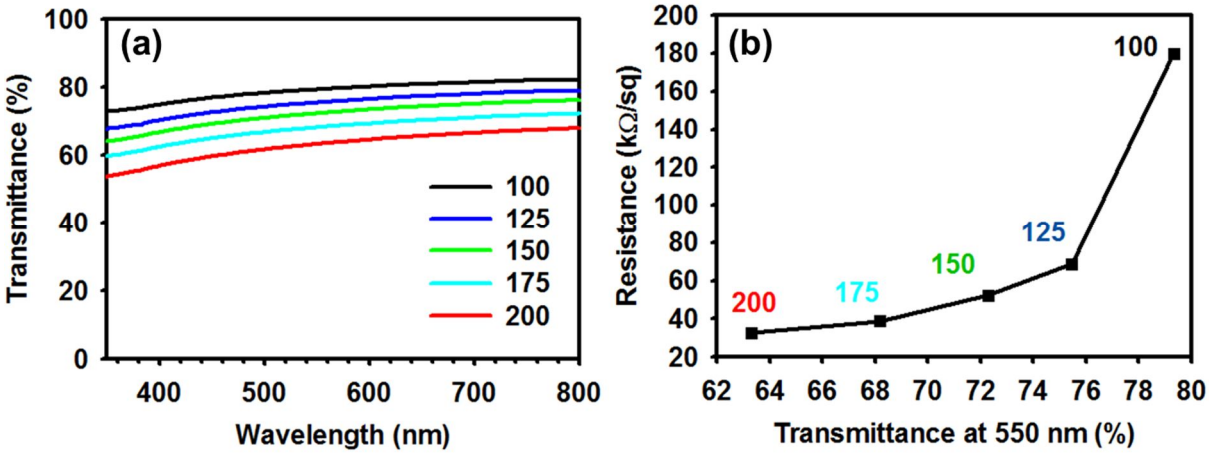

Figure 20. (a) Optical transmittance of spray coated SHPEK-g-MWCNT on PET films; (b) sheet resistance with respect to number of spray coatings.

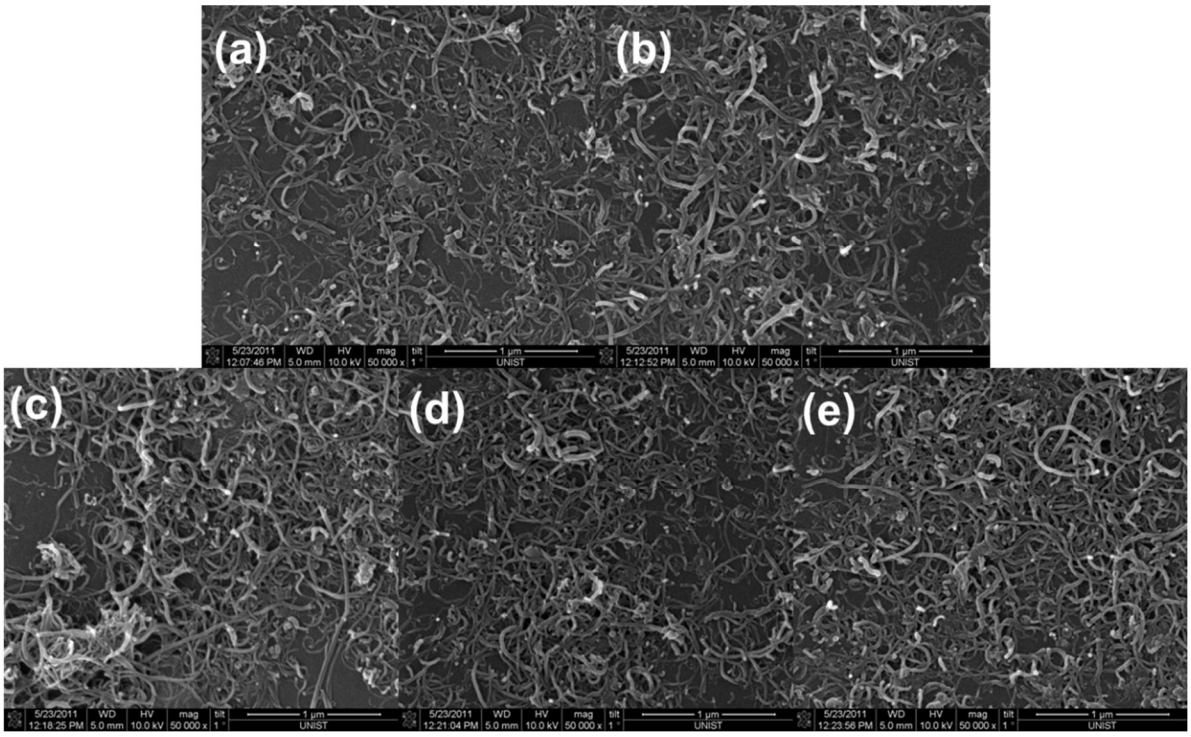

Figure 21. SEM images from the top view of (a) 100 spray coatings; (b) 125 spray coatings; (c) 150 spray coatings; (d) 175 spray coatings; (e) 200 spray coatings. (50,000x).

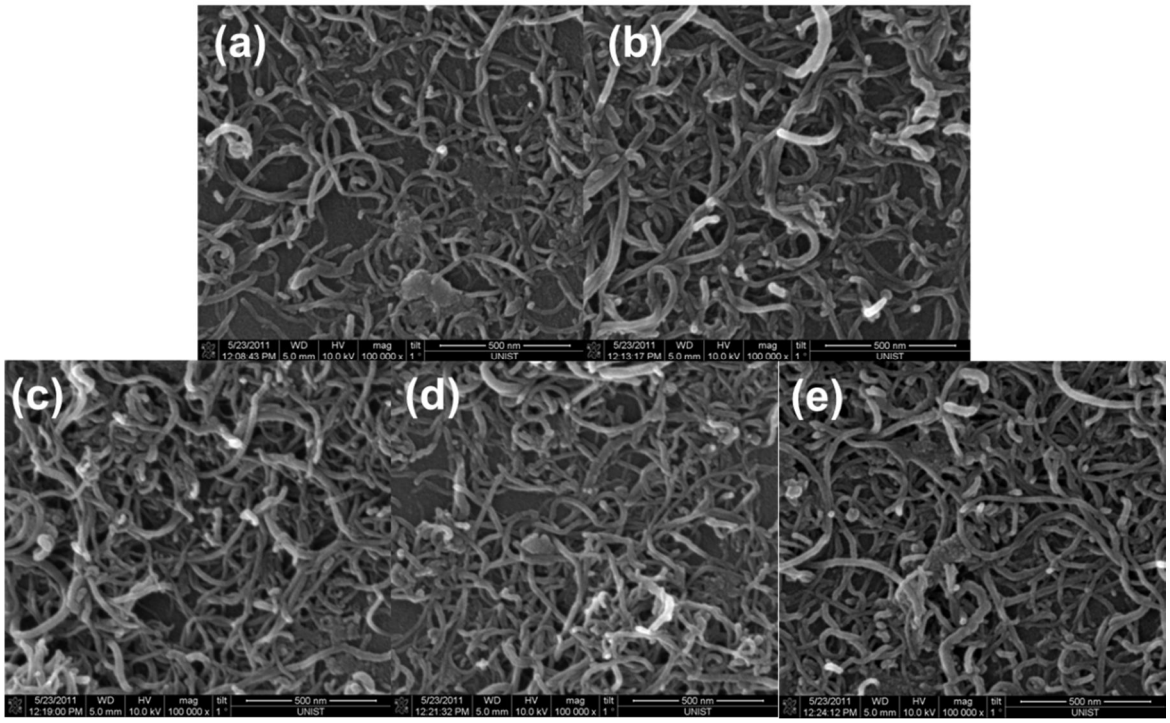

Figure 22. SEM images from the top view of (a) 100 spray coatings; (b) 125 spray coatings; (c) 150 spray coatings; (d) 175 spray coatings; (e) 200 spray coatings. (100,000x)

3.10 Electrical Conductivity of Films

Having structural confirmation and solubility information, freestanding SHPEK-g-MWCNT papers were also prepared by a simple filtration of the dispersed solution in water through cellulose membrane (0.2 μm of pore size) (Figure 23a). After filtration, membrane was removed by using NMP (Figure 23b) and freestanding MWCNT film successfully Depending on the amounts of SHPEK-g-MWCNT at given diameter (1.5 cm), sheet resistance was reduced to as low as 63 Ω/sq (Figure 23c). The low sheet resistance should be originated from low percolation threshold of SHPEK-g-MWCNT, which has high aspect ratio even after grafting and sulfonation in non-destructive medium. To our best knowledge, this work is the first time demonstration of freestanding MWCNT paper prepared from water dispersible MWCNT without chemical oxidation.[29]

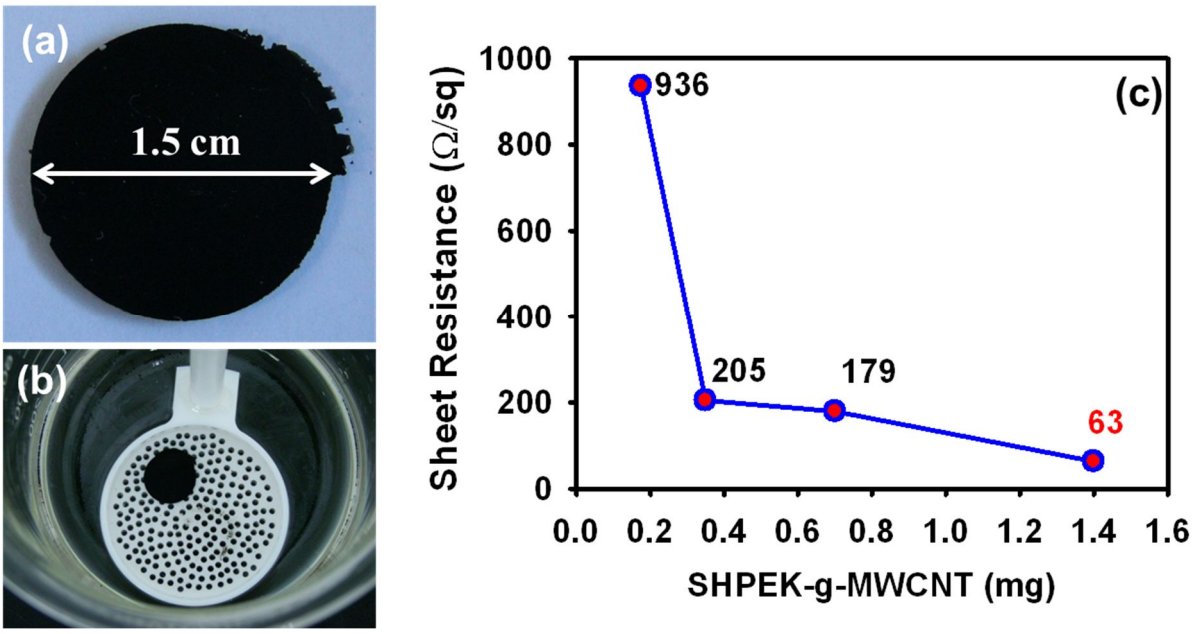

Figure 23. (a) Photograph of freestanding SHPEK-g-MWCNT film (1.5 cm) prepared from filtration of SHPEK-g-MWCNT solution in water; (b) Removing cellulose membrane in NMP. (c) Sheet resistance changes as a function of SHPEK-*g*-MWCNT weight at given diameter.

3.11 Cyclic voltammetry

In addition to low sheet resistance (high electrical conductivity), which is prerequisite for high performance electrode, a large number of sulfonic acids on its periphery make SHPEK-g-MWCNT hydrophilic to efficiently adsorb oxygen.[30] SHPEK-g-MWCNT is thus expected to display a good electrocatalytic activity for oxygen reduction reaction (ORR). Hence, the SHPEK-g-MWCNT (0.5 mg) solution in DMAc (1.5 mL) was drop-coated on a glassy carbon (GC) electrode. For comparison, HPEK-g-MWCNT on GC (HPEK-g-MWCNT/GC) electrode was also prepared at the same condition. Pristine MWCNT and Pt/C (Commercially available electrolyte) also measured as references. Although the SHPEK-g-MWCNT showed profoundly higher capacitance than that of HPEK-g-MWCNT (Figure 24a), featureless voltammetric currents from both electrodes were observed in N_2 saturated 0.1 M aqueous KOH solution within the potential range of -1.0-0.2 V. On the other hand, in O_2 saturated solution, HPEK-g-MWCNT and SHPEK-g-MWCNT/GC electrodes displayed dramatic increase in voltametric current more than 26 and 14 times (Figure 24b), respectively, compared to the current observed in N_2 saturated electrolyte. The results indicated that both HPEK-g-MWCNT and SHPEK-g-MWCNT have high electrocatalytic activity for ORR, but the latter is more significantly efficient due to its much higher hydrophilicity. On-set potential of ORR for HPEK-g-MWCNT is -0.24 V, which is slightly higher than that (-0.20 V) commercially available Platinum (Pt) on activated carbon (Pt/C, Vulcan XC-72R). On the other hand, SHPEK-g-MWCNT displayed its on-set potential at -0.16 V, suggesting that its electrocatalytic activity is superior to Pt-based catalysts. Specific capacitance is dramatically increased in O_2 saturated 0.1M KOH solution and even higher than Pt/C (Figure 24b and Table 4). We also investigated the electrochemical stability of HPEK-g-MWCNT/GC and SHPEK-g-MWCNT/GC electrodes. These samples also showed good stability in N_2, O_2 saturated 0.1M KOH solution. After 100^{th} cycle, the shape of electrocatalytic activity curve remains its original shape similar with 10^{th} cycle (Figure 25, 26)

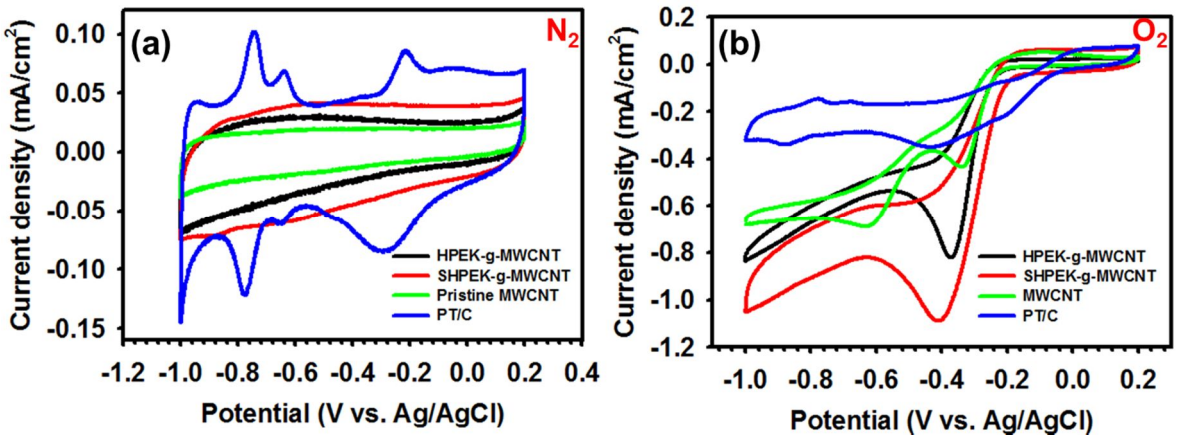

Figure 24. Cyclic voltammograms of sample films on glassy carbon (GC) electrodes in 0.1 M aqueous KOH solution with a scan rate of 0.1 V/s: (c) N_2 saturated; (d) O_2 saturated.

Table 4. Capacitance of samples/GC electrodes.

Capacitance (F/g)		
Sample Name	N_2 saturated	O_2 saturated
HPEK-g-MWCNT	36.12	68.03
SHPEK-g-MWCNT	54.78	150.99
Pristine MWCNT	22.45	59.92
Pt/C	81.03	85.15

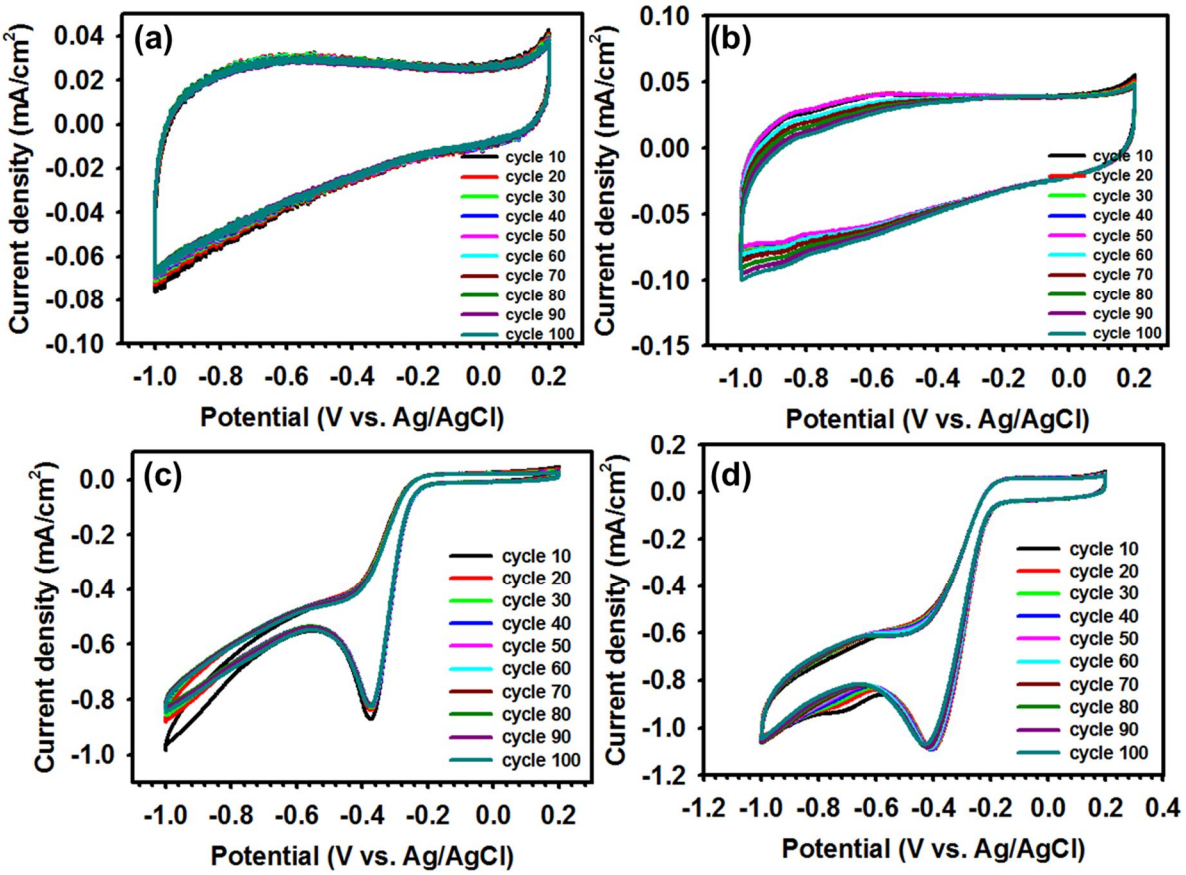

Figure 25. Cyclic voltammograms in 0.1 M aqueous KOH solution with a scan rate of 10 mV/s of : (a) HPEK-g-MWCNT and (b) SHPEK-g-MWCNT on glassy carbon (GC) electrodes in N_2 saturated and (c) HPEK-g-MWCNT (d) SHPEK-g-MWCNT on glassy carbon (GC) electrodes in O_2.

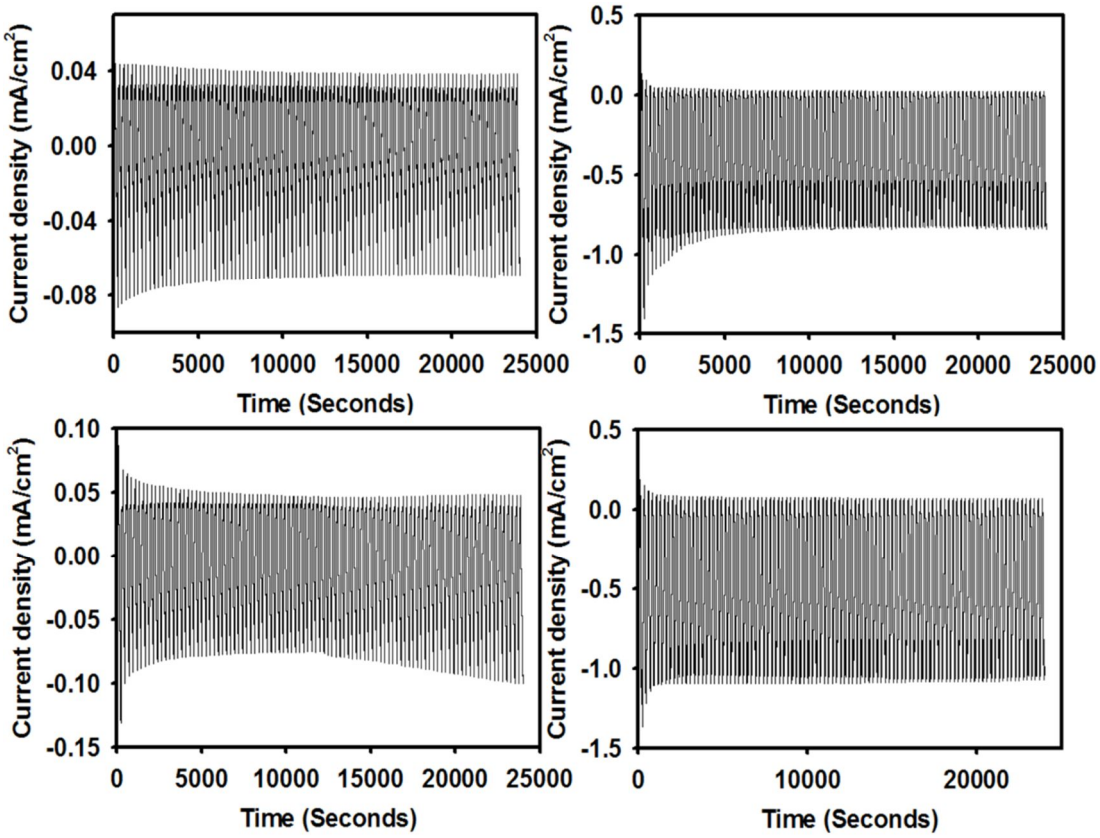

Figure 26. Electrochemical stability in 0.1 M aqueous KOH solution with a scan rate of 10 mV/s of : (a) HPEK-g-MWCNT and (b) SHPEK-g-MWCNT on glassy carbon (GC) electrodes in N_2 saturated and (c) HPEK-g-MWCNT (d) SHPEK-g-MWCNT on glassy carbon (GC) electrodes in O_2.

IV. Conclusions

Multi-wall carbon nanotubes (MWCNTs) have inherent sp^2 hybrid C-H defects for the electrophilic substitution reaction. To introduce abundant reactive sites to the surface of MWCNT without further oxidative damages, dendritic hyperbranched poly(ether-ketone) (HPEK) was grafted onto the surface of MWCNT to produce HPEK grafted MWCNT (HPEK-g-MWCNT). The HPEK-g-MWCNT could provide a numerous activated sites for subsequent sulfonation to afford sulfonated HPEK-g-MWCNT (SHPEK-g-MWCNT). The covalent grafting and sulfonation of MWCNT were confirmed with a various analytical techniques. The resultant SHPEK-g-MWCNT was dispersible well in water with Zeta potential of -57.8 mV (good stability). Freestanding SHPEK-g-MWCNT paper displays sheet resistance as low as 63 Ω/sq and high electrocatalytic activity for oxygen reduction reaction (ORR). Hence, the approach is a unique wet-chemical functionalization route that does not require initial oxidative damage onto MWCNT framework. Water-dispersible SHPEK-g-MWCNT can be processed by a simple spray coating for uses in a various applications such as biological technologies, fuel cells, batteries, sensors and opto-electronics in practice.

References

1. (a) EBBESEN, T. W., LEZEC, H.J., HIURA, H., BENNETT, J. W.,GHAEMI, H. F., & THIO, T. 1996. Electrical conductivity of individual carbon nanotubes. *Nature*, 382, 54-56. (b) IIJIMA, S. 1991. Helical microtubules of graphitic carbon. *Nature*, 354, 56-58. (c) JIN, Z., PRAMODA, K. P., XU, G. & GOH, S. H. 2001. Dynamic mechanical behavior of melt-processed multi-walled carbon nanotube/poly (methyl methacrylate) composites. *Chemical Physics Letters*, 337, 43-47. (d) TREACY, M. M. JEBBESSEN, T. W. & GIBSON, J. M. 1996. Exceptionally high Young's modulus observed for individual carbon nanotubes. *Nature*, 381, 678-680.

2. MONIRUZZAMAN, M., WINEY, K. I. 2006. Polymer nanocomposites containing carbon nanotubes. *Macromolecules*, 39, 5194-5205

3. FRACKOWIAK, E., BEQUIN, F. 2001. Carbon materials for the electrochemical storage of energy in capacitors. *Carbon* , 39, 937-950.

4. ANANTRAM, M. P., LEONARD, F. 2006. Physics of carbon nanotube electronic devices. *Reports on Progress in Physics*, 69, 507-561.

5. WANG, J. 2005. Carbon-nanotube based electrochemical biosensors: A review. *Electroanalysis*, 17, 7-14.

6. (a) BAUGHMAN, R. H., ZAKHIDOV, A. A. & DE HEER, W. A. 2002. Carbon nanotubes--the route toward applications. *Science*, 297, 787-792. (b) LIU, Z., SUN, X., NAKAYAMA-RATCHFORD, N. & DAI, H. 2007. Supramolecular chemistry on water-soluble carbon nanotubes for drug loading and delivery. *ACS Nano*, 1, 50-56.

7. (a) JIN, L., BOWER, C. & ZHOU, O. 1998. Alignment of carbon nanotubes in a polymer matrix by mechanical stretching. *Applied physics letters*, 73, 1197-1199 (b) ANDREWS, R., JACQUES, D., RAO, A., RANTELL, T., DERBYSHIRE, F., CHEN, Y., CHEN, J. & HADDON, R. 1999. Nanotube composite carbon fibers. *Applied physics letters*, 75, 1329-1331. (c) SHAFFER, M. S. P. & WINDLE, A. H. 1999. Fabrication and characterization of carbon nanotube/poly (vinyl alcohol) composites. *Advanced Materials*, 11, 937-941. (d) CHEN, G. Z., SHAFFER, M. S. P., COLEBY, D., DIXON, G., ZHOU, W., FRAY, D. J. & WINDLE, A. H. 2000. Carbon nanotube and polypyrrole composites: coating and doping. *Advanced Materials*, 12, 522-526.

8. (a) DAI, L. & MAU, A. W. H. 2001. Controlled Synthesis and Modification of Carbon Nanotubes and C~ 6~ 0: Carbon Nanostructures for Advanced Polymeric Composite Materials. *Advanced Materials*, 13, 899-913. (b) HIRSCH, A. 2002. Functionalization of single-walled carbon nanotubes. *Angewandte Chemie International Edition*, 41, 1853-1859.
(c) SUN, Y. P., FU, K., LIN, Y. & HUANG, W. 2002. Functionalized carbon nanotubes: properties and applications. *Accounts of chemical research*, 35, 1096-1104.

9. (a) HUANG, W., LIN, Y., TAYLOR, S., GAILLARD, J., RAO, A. M. & SUN, Y. P. 2002. Sonication-assisted functionalization and solubilization of carbon nanotubes. *Nano Letters*, 2, 231-234. (b) KUMAR, S., DANG, T. D., ARNOLD, F. E., BHATTACHARYYA, A. R., MIN, B. G., ZHANG, X., VAIA, R. A., PARK, C., ADAMS, W. W. & HAUGE, R. H. 2002. Synthesis, Structure, and Properties of PBO/SWNT Composites[&]. *Macromolecules*, 35, 9039-9043.

10. (a) SUSLICK, K. S. 1990. Sonochemistry. *Science*, 247, 1439-1445. (b) SUSLICK, K. S., GAWIENOWSKI, J. J., SCHUBERT, P. F. & WANG, H. H. 1983. Alkane sonochemistry. *The Journal of Physical Chemistry*, 87, 2299-2301.

11. (a) ZHANG, Y., SHI, Z., GU, Z. & IIJIMA, S. 2000. Structure modification of single-wall carbon nanotubes. *Carbon*, 38, 2055-2059. (b) MONTHIOUX, M., SMITH, B., BURTEAUX, B., CLAYE, A., FISCHER, J. & LUZZI, D. 2001. Sensitivity of single-wall carbon nanotubes to chemical processing: an electron microscopy investigation. *Carbon*, 39, 1251-1272. (c) SALZMANN, C. G., LLEWELLYN, S. A., TOBIAS, G., WARD, M. A. H., HUH, Y. & GREEN, M. L. H. 2007. The Role of Carboxylated Carbonaceous Fragments in the Functionalization and Spectroscopy of a Single-Walled Carbon-Nanotube Material. *Advanced Materials*, 19, 883-887.

12. (a) BRODIE, B. 1860. Sur le poids atomique du graphite. *Annales des Chimie et des Physique*, 59, 466-472. (b) STAUDENMAIER, L. 1898. Verfahren zur darstellung der graphitsäure. *Berichte der deutschen chemischen Gesellschaft*, 31, 1481-1487. (c) HUMMERS JR, W. S. & OFFEMAN, R. E. 1958. Preparation of graphitic oxide. *Journal of the American Chemical Society*, 80, 1339-1339.

13. PARK, S. & RUOFF, R. S. 2009. Chemical methods for the production of graphenes. *Nature nanotechnology*, 4, 217-224.

14. (a) NOVOSELOV, K., GEIM, A., MOROZOV, S., JIANG, D., ZHANG, Y., DUBONOS, S., GRIGORIEVA, I. & FIRSOV, A. 2004. Electric field effect in atomically thin carbon films. *Science*, 306, 666-669. (b) GEIM, A. K. & NOVOSELOV, K. S. 2007. The rise of graphene. *Nature materials*, 6, 183-191.

15. BAEK, J. B., LYONS, C. B. & TAN, L. S. 2004. Covalent modification of vapour-grown carbon nanofibers via direct Friedel–Crafts acylation in polyphosphoric acid. *Journal of Materials Chemistry*, 14, 2052-2056.

16. LEE, H. J., HAN, S. W., KWON, Y. D., TAN, L. S. & BAEK, J. B. 2008. Functionalization of multi-walled carbon nanotubes with various 4-substituted benzoic acids in mild polyphosphoric acid/phosphorous pentoxide. *Carbon*, 46, 1850-1859.

17. Fréchet, J. M. J. 1994. Functional polymers and dendrimers: reactivity, molecular architecture, and interfacial energy. *Science*, 263, 1710-1715.

18. PALONIEMI, H., Ä RITALO, T., LAIHO, T., LIUKE, H., KOCHAROVA, N., HAAPAKKA, K., TERZI, F., SEEBER, R. & LUKKARI, J. 2005. Water-soluble full-length single-wall carbon nanotube polyelectrolytes: preparation and characterization. *The Journal of Physical Chemistry B*, 109, 8634-8642.

19. ZHAO, B., HU, H., YU, A., PEREA, D. & HADDON, R. C. 2005. Synthesis and characterization of water soluble single-walled carbon nanotube graft copolymers. *Journal of the American Chemical Society*, 127, 8197-8203.

20. SHIN, Y. R., JEON, I. Y. & BAEK, J. B. 2011. Stability of multi-walled carbon nanotubes in commonly used acidic media. *Carbon*, Doi:10.1016/j.carbon.2011.11.017

21. SHU, C. F., LEU, C. M. & HUANG, F. Y. 1999. Synthesis, modification, and characterization of hyperbranched poly (ether ketones). *Polymer*, 40, 6591-6596.

22. American Society for Testing and Materials 1985. Zeta Potential of Colloids in Water and Waste Water, 1985. ASTM Standard D 4187-82.

23. JIANG, L., GAO, L. & SUN, J. 2003. Production of aqueous colloidal dispersions of carbon nanotubes. *Journal of colloid and interface science*, 260, 89-94.

24. LI, D., M LLER, M. B., GILJE, S., KANER, R. B. & WALLACE, G. G. 2008. Processable aqueous dispersions of graphene nanosheets. *Nature nanotechnology*, 3, 101-105.

25. WELLISCH, E., GIPSTEIN, E. & SWEETING, O. J. 1962. Thermal Decomposition of Sulfinic Acids1. *The Journal of Organic Chemistry*, 27, 1810-1812.

26. SORESCU, D. C., JORDAN, K. D. & AVOURIS, P. 2001. Theoretical study of oxygen adsorption on graphite and the (8, 0) single-walled carbon nanotube. *The Journal of Physical Chemistry B*, 105, 11227-11232.

27. BOURG, M. C., BADIA, A. & LENNOX, R. B. 2000. Gold-sulfur bonding in 2D and 3D self-assembled monolayers: XPS characterization. *The Journal of Physical Chemistry B*, 104, 6562-6567.

28. KRUEGER, B. J., GRASSIAN, V. H., IEDEMA, M. J., COWIN, J. P. & LASKIN, A. 2003. Probing heterogeneous chemistry of individual atmospheric particles using scanning electron microscopy and energy-dispersive X-ray analysis. *Analytical Chemistry*, 75, 5170-5179.

29. HAN, J. T., KIM, S. Y., WOO, J. S., JEONG, H. J., OH, W. & LEE, G. W. 2008. Hydrogen-bond-driven assembly of thin multiwalled carbon nanotubes. *The Journal of Physical Chemistry C*, 112, 15961-15965.

30. YU, D., NAGELLI, E., DU, F. & DAI, L. 2010. Metal-free carbon nanomaterials become more active than metal catalysts and last longer. *The Journal of Physical Chemistry Letters*, 1, 2165-2173.

Manuscript

Domestic

1. Gyung-Joo Sohn, In-Yup Jeon and Jong-Beom Baek "**Sulfonated Hyperbranched Poly (ether-ketone) Grafted MWNT**" Recent Progress in Graphene Research 2011 (Suwon, October 3-6)
2. Dong Wook Chang, Gyung-Joo Sohn, Liming Dai and Jong-Beom Baek "**Reversible adsorption of conjugated amphiphilic dendrimers onto reduced graphene oxide (rGO) for fluorescence sensing**" The polymer Society of Korea 2011, 36(2), (Gwangju, October 6-7)
3. Gyung-Joo Sohn, In-Yup Jeon, Jong-Beom Baek "**Functionalization of graphite with polyether-ketones and successive sulfonation**" The polymer Society of Korea 2011, 36(1), (Daejeon, April 7-8).
4. Gyung-Joo Sohn, In-Yup Jeon, Jong-Beom Baek "**Sulfonated Hyperbranched Poly(ether-ketone) Grafted MWNT**" The polymer Society of Korea 2010, 35(2), (Daegu, October 7-8).
5. Gyung-Joo Sohn, In-Yup Jeon, Jong-Beom Baek "**Synthesis of Water Soluble Carbon Nanotubes by Sulfonation**." The polymer Society of Korea 2010, 35(1), (Daejeon, April 8-9)